A Macroscopic Description of Lipid Bilayer Phase Transitions of Mixed-Chain Phosphatidylcholines: Chain-Length and Chain-Asymmetry Dependence

Lubin Chen, Michael L. Johnson, and Rodney L. Biltonen
Department of Pharmacology and the Biophysics Program, University of Virginia Health System, Charlottesville, Virginia 22908 USA

ABSTRACT A macroscopic model is presented to quantitatively describe lipid bilayer gel to fluid phase transitions. In this model, the Gibbs potential of the lipid bilayer is expressed in terms of a single order parameter q, the average chain orientational order parameter. The Gibbs potential is based on molecular mean-field and statistical mechanical calculations of inter and intrachain interactions. Chain-length and chain-asymmetry are incorporated into the Gibbs potential so that one equation provides an accurate description of mixed-chain phosphatidylcholines of a single class. Two general classes of lipids are studied in this work: lipid bilayers of partially or noninterdigitated gel phases, and bilayers of mixed interdigitated gel phases. The model parameters are obtained by fitting the transition temperature and enthalpy data of phosphatidylcholines to the model. The proposed model provides estimates for the transition temperature and enthalpy, van der Waals energy, number of *gauche* bonds, chain orientational order parameter, and bond rotational and excluded volume entropies, achieving excellent agreement with existing data obtained with various techniques.

INTRODUCTION

The major structural component of biomembranes is the lipid bilayer, which not only serves as a permeability barrier, but modulates the activities of embedded proteins and anchored glycoproteins through its collective physical properties (Singer and Nicolson, 1972; Biltonen, 1990; Mouritsen and Biltonen, 1993). One potentially important property of the lipid bilayer is the tendency of chemically or structurally similar lipids to cluster (or phase separate) within the plane of the bilayer (Huang et al., 1993c; Jørgensen and Mouritsen, 1995; Jerala et al., 1996). This clustering can, in turn, promote localization or colocalization of reactive components altering the potential for protein-protein interaction, rates of reaction, and diffusion rates (Thompson et al., 1995; Dibble et al., 1996; Hinderliter et al., 1997; Gil et al., 1998; Sabra and Mouritsen, 1998). The physical basis of this type of functional modulation can be traced, in part, to differences in the energetics of interactions between chemically or structurally distinct lipids (Hønger et al., 1996; Hinderliter et al., 1998; Sugár et al., 1999). Thus the development of an understanding of the relationship between lipid structure and membrane function requires knowledge of the magnitude of these interactions and their structural consequences. The purpose of this study is to establish a macroscopic description of the gel-fluid phase transition in thermodynamic and structural terms of two general classes of lipids as a step in that direction.

Model systems consisting of a few natural or synthetic phospholipids are well defined and can be conveniently studied by physical techniques and theories to gain information on bilayer properties (Melchior and Stein, 1976; Mabrey and Sturtevant, 1978; Seelig and Seelig, 1980; Jørgensen and Mouritsen, 1995; McMullen et al., 1999; Korlach et al., 1999). The gel to fluid or main phase transition has been a major focus of lipid research for decades (Cevc and Marsh, 1987). Since phosphatidylcholines (PCs) are the most abundant lipids in biomembranes and widely used in model membrane studies, there is a large body of information available (Koynova and Caffrey, 1998). In the past two decades, considerable experimental work has been performed on mixed-chain PCs with different acyl chains at the *sn*-1 and *sn*-2 positions (Huang and Li, 1999).

It was suggested (Mason et al., 1981; Huang et al., 1983) that when the chain mismatch of the two chains exceeds ~3 methylene units, the bilayer forms a partially interdigitated gel phase (shown schematically in Fig. 1 *A*). In such a phase the mismatched region of one leaflet is matched with that of the other leaflet, so that the bilayer thickness is approximately the sum of the lengths of the two acyl chains and the area/lipid is about twice the area/chain. As the chain asymmetry increases to the point that the length of the longer chain is about twice that of the shorter one, the bilayer forms a mixed interdigitated gel phase (shown schematically in Fig. 1 *B*). In this phase the mismatched region of one leaflet is matched with the shorter chain of the other leaflet so that the bilayer thickness is approximately the length of the longer chain, and the area/lipid is about three times the area/chain (McIntosh et al., 1984; Hui et al., 1984). Other studies (Shah et al., 1990; Halladay et al., 1990; Lewis et al., 1994b; Zhu and Caffrey, 1994) further suggested that the mixed interdigitated gel phase undergoes a transformation to the partially interdigitated fluid phase at the phase tran-

Received for publication 22 September 1999 and in final form 27 September 2000.

Address reprint requests to Dr. Rodney L. Biltonen, Dept. of Pharmacology, University of Virginia, Charlottesville, VA 22908. Tel.: 804-924-2422; Fax: 804-982-0569; E-mail: biltonen@virginia.edu.

0006-3495/01/01/254/17 $2.00

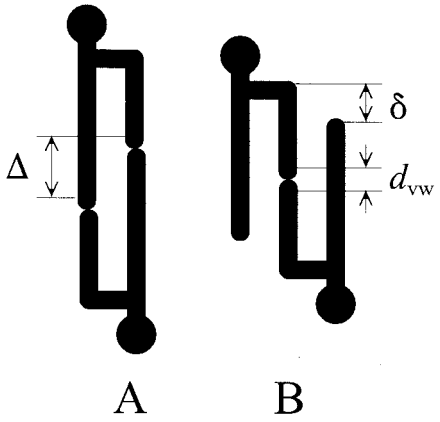

FIGURE 1 Schematic diagram to show two lipid bilayer packing structures and their associated structural quantities. (*A*) Partial interdigitation; (*B*) mixed interdigitation.

sition temperature. Huang and co-workers have developed empirical equations to correlate the transition temperatures to chain properties for lipid bilayers existing in non, partially, and mixed interdigitated gel states (Huang, 1991; Huang et al., 1993a, b; Li et al., 1994). Marsh (1992, 1999) attempted to provide some thermodynamic understanding of the work of Huang and co-workers by analyzing the transition temperature data assuming the transition enthalpy and entropy changes to be linear functions of chain-length and chain-asymmetry.

A number of theoretical models have been proposed to gain insight into the mechanism of lipid bilayer gel-fluid phase transitions and to interpret experiments (Nagle, 1980; Caillé et al., 1980; Pink, 1982; Cevc and Marsh, 1987). Models that are microscopic in nature include lattice models (Nagle, 1973; Doniach, 1978; Pink et al., 1980), molecular mean-field models (Marčelja, 1974; Meraldi and Schlitter, 1981a, b), Monte Carlo simulations (Mouritsen et al., 1983, 1992; Sugár et al., 1999), and molecular dynamics simulations (van der Ploeg and Berendsen, 1982; Tu et al., 1995). Models that are macroscopic in nature include variations of Landau theory (Owicki et al., 1978; Priest, 1980; Jähnig, 1981), assuming the Gibbs free energy to be a polynomial of some order parameter. These theoretical models only provide descriptions of lipids with identical acyl chains.

The goal of the current work is to present a macroscopic model to describe the chain-length and chain-asymmetry dependence of lipid bilayer gel-fluid phase transitions. The model parameters are obtained by fitting the transition temperature and enthalpy data of selected PCs to the model so that the model can accurately represent the data. The model is tested by the comparison of its predictions with the transition temperature and enthalpy data of other PCs not used in the fitting procedure. The model also provides macroscopic estimates of other thermodynamic and structural quantities such as interchain van der Waals energy, number of *gauche* conformers, chain orientational order parameter, and bond rotational and excluded volume entropies. The agreement between model calculations and existing data obtained with various techniques provides a further test of the accuracy of the model and its parameters. Where experimental information is not yet available, the model provides estimates of unknown quantities. The model is derived from and applied to saturated lipids only, but can be easily modified to account for biological lipids that are unsaturated. This work is inspired by the classic van der Waals theory on liquid-gas phase transitions.

THE THEORETICAL MODEL

A spontaneously formed lipid bilayer in excess water is a complicated structure, even for a single component system. A large number of intra and intermolecular interactions of lipid-lipid and lipid-water need to be considered. These include headgroup electrostatic interactions, hydration, and steric interactions, van der Waals attraction between chains, hard-core repulsions between chains and between different segments of chains, and *trans-gauche* isomerization of chain segments. In order to provide a description of lipid bilayers, it is necessary to approximate the important interactions and ignore the minor ones, as has been done in a large number of theoretical models on lipid bilayers. The most important interactions are the hard-core repulsion or excluded volume interaction, van der Waals attraction, *trans-gauche* isomerization, and headgroup steric interactions. The thermodynamic quantities describing these interactions in lipid bilayers are assumed to be related to a single-order parameter.

The order parameter

Since the lipid bilayer has a preferred axis, the bilayer normal, the motion of lipid chains, is anisotropic. Let **n** denote the unit vector along the bilayer normal. Following Seelig and coworkers (Seelig and Niederberger, 1974; Seelig and Seelig, 1974), a vector, **v,** is assigned to each chain segment, whose direction is given by the normal to the plane spanned by the two C–H bonds so that when the chain is in an untilted all-*trans* crystal state, **v** is coincident with **n** and its length is a (= 1.27 Å), the projection of one C–C bond on the bilayer normal. When the chain is in motion, **v** makes an instantaneous angle θ with **n**. The segmental order parameter, Q, is defined as the time average of the second Legendre polynomial, $Q = (3\langle\cos^2\theta\rangle - 1)/2$ and can be calculated from deuterium NMR measurements as $Q = -2S_{CD}$, where S_{CD} is the order parameter of a C–D bond associated with the segment (Seelig and Niederberger, 1974). Q has been shown to vary along the lipid chain (Seelig and Seelig, 1974).

The above description is microscopic in nature. Having a preferred axis, the lipid bilayer may be treated as a uniaxial system from a thermodynamic point of view. Such a uniaxial system can be characterized by a single-order parameter (de Gennes, 1971). To macroscopically describe the lipid bilayer phase transition, we define a chain orientational order parameter, q, as the arithmetic average of the segmental order parameter Q_i along the chain. This is equivalent to assigning a vector to the chain as having an angle θ with **n,** where $\cos^2\theta$ is calculated as the average of segmental $\cos^2\theta_i$, even for a flexible chain, so that we can write

$$q = \frac{1}{2}(3\langle\cos^2\theta\rangle - 1) \tag{1a}$$

$$\langle\cos^2\theta\rangle = \frac{1}{n_s}\sum_{i=1}^{n_s}\langle\cos^2\theta_i\rangle \tag{1b}$$

where n_s is the number of segments in the chain (brackets denote the time average in this work). $q = 0$ represents the chain in a completely random state and $q = 1$ in an untilted perfect crystal state, so that q retains the meaning of a normalized order parameter.

The thermodynamic potential

Starting with the molecular mean-field theory of Meraldi and Schlitter (1981a, b) and the statistical mechanical calculation of Priest (1980), the Gibbs potential of lipid bilayers is:

$$G = H - TS = W_s + U_g + U_{vw} - T(S_g + S_{pk}) \quad (2a)$$

$$W_s = \pi A \quad (2b)$$

$$U_g = E_g n_g = E_g(N_c - 6)f_g \quad (2c)$$

$$S_g/R = (N_c - 4)s_g(f_g) \quad (2d)$$

$$U_{vw} = -\frac{1}{2}(B_0 + B_2 q^2)\sigma^2 \quad (2e)$$

$$S_{pk}/R = -(C_0 - C_2 q^2)\sigma^2 \quad (2f)$$

where G, H, S, T, and R are the Gibbs potential, enthalpy, entropy, absolute temperature, and gas constant; W_s accounts for steric and hydrophobic interactions imposed on the headgroup packing (originally introduced by Marčelja, 1974): π is the lateral surface pressure and A the area/lipid; U_g and S_g are the energy and entropy contributions (Priest, 1980), respectively, due to *gauche* bond formation; E_g is the energy of a single *gauche* bond relative to that of a *trans* bond, n_g the number of *gauche* bonds per molecule, f_g the fraction of *gauche* bonds, N_c the total number of carbons of the molecule, and s_g the entropy contribution per bond; U_{vw} and S_{pk}, respectively, are the energy and entropy contributions of van der Waals attractions and hard-core repulsions (excluded volume or packing) based on the work of Meraldi and Schlitter (1981a, b). [In the work of Meraldi and Schlitter (1981a,b), each segment was treated individually so that U_{vw} and S_{pk} were summed over all segments. Meraldi and Schlitter adapted the work of Cotter (1977) and Gelbart and Baron (1977) on nematic liquid crystals to flexible lipid chains. It should also be mentioned that in the calculations to be described, all energy terms are in the units per mole of lipid. The numerical values of some quantities are given in other units (rather than in molar units) only for convenience of communication.] The chain orientational order parameter defined above is indicated by q; B_0, B_2, C_0, and C_2 are chain-length-dependent positive coefficients and are treated in detail in the section on chain-length and chain-asymmetry dependence; σ is a factor, originally introduced by Marčelja (1974) in his molecular mean-field theory as the ratio of the number of *trans* bonds to the total number of bonds in a chain. Based on Salem's calculation (1962) of interchain van der Waals interactions, Pink and co-workers (Pink et al., 1980; Pink, 1982) pointed out that σ^2 should be inversely proportional to the 5th power of interchain distance. The interchain distance is equal to the chain diameter and is proportional to the square root of the area/lipid, A. When the untilted all-*trans* chain in the crystal state is taken as the reference with area/lipid, A_0, one obtains $\sigma^2 = (A_0/A)^{5/2}$. It should be emphasized that all quantities in Eq. 2 are macroscopic averages (e.g., q is averaged over all chains), so that all molecules are treated equally.

To make Eq. 2 useful for the studies of lipid bilayer main phase transitions, we postulate that lipid bilayer gel-fluid phase transitions can be characterized by the single-order parameter, q, as previously described. If the volume is assumed to remain constant, $A \cdot l = A_0 \cdot l_0$, where l is the (time-averaged) chain-length projection on the bilayer normal and l_0 that of the all-*trans* extended chain in the crystal state. $l = \langle \Sigma \mathbf{v}_i \cdot \mathbf{n} \rangle = n_s a(1/n_s)\Sigma\langle\cos\theta_i\rangle = l_0(1/n_s)\Sigma\langle\cos\theta_i\rangle$, so that

$$\frac{l}{l_0} = \frac{1}{n_s}\sum_{i=1}^{n_s}\langle\cos\theta_i\rangle \quad (3)$$

which is the arithmetic average of $\langle\cos\theta_i\rangle$. However, Eq. 1b is the average of $\langle\cos^2\theta_i\rangle$. Generally, these two averaging processes will give different results. However, if all $\langle\cos\theta_i\rangle \geq 0$, one expects the square root of Eq. 1b to be a good approximation to Eq. 3, so that

$$\frac{l}{l_0} = \frac{A_0}{A} = r(q) = \sqrt{\frac{2q+1}{3}} \quad (4)$$

The assumption that $\langle\cos\theta_i\rangle \geq 0$ means that in the time-averaged sense, $\theta_i \leq 90°$. In other words, we ignore the possibility of loop conformations in acyl chains, which is probably reasonable except for chain termini. If all $\cos\theta_i$ are the same and equal to $\cos\theta$, Eq. 4 becomes $\langle\cos\theta\rangle = \sqrt{\langle\cos^2\theta\rangle}$. Thus, the angular fluctuations, $(\langle\cos^2\theta\rangle - \langle\cos\theta\rangle^2) > 0$, are neglected, so that Eq. 4 is the upper limit of estimates of l/l_0 (see Discussion).

To relate f_g to q, we consider the two extreme conditions: at $q = 0$, S_g is maximal and at $q = 1$, $S_g = 0$. However, when $f_g = 1/2$, S_g is maximal (Priest, 1980) and at $f_g = 0$, $S_g = 0$. The simplest relationship satisfying these two extreme conditions (see Discussion) is

$$f_g(q) = (1 - q)/2 \quad (5)$$

With Eq. 5, the entropy contribution per bond, s_g, can be expressed as

$$s_g(q) = \frac{1}{2}(1+q)\ln\left(\frac{1 - q + \sqrt{2q^2+2}}{1+q}\right) + \frac{1}{2}(1-q)\ln\left(\frac{1+q+\sqrt{2q^2+2}}{1-q}\right) \quad (6)$$

which was obtained by Priest (1980, where a factor of 1/2 was missing) using a transfer matrix method following Flory (1969). It should be noted that Eq. 6 is strictly valid only in the limit of infinitely long chains.

Chain-length and chain-asymmetry dependence

First, we would like Eq. 2 to describe a class of saturated lipids that form partially or noninterdigitated (PI) gel phases. This is inspired by Huang's empirical formulation that correlates the transition temperatures of this class of PCs to chain properties (Huang, 1991; Huang et al., 1993a; 1994). Two structural quantities for C(X)C(Y)PC, where X and Y are the number of carbons in *sn*-1 and *sn*-2 chains, respectively, are defined as:

$$N = X - 1 + Y - 1 - 1 = X + Y - 3 \quad (7a)$$

$$\Delta = X - 1 - (Y - 1 - d_{12}) = X - Y + d_{12} \quad (7b)$$

where N is the total number of C–C bonds participating in interchain interactions, Δ is the number of mismatched bonds between the two chains, and d_{12} the inherent shortening of the *sn*-2 chain. Being approximately parallel to the bilayer surface, the first bond of the *sn*-2 chain is assumed to make no contribution to interchain interactions and is responsible for the shortening of the *sn*-2 chain.

B_0 and B_2 are related to the van der Waals interaction strength and assumed to be proportional to $N - N_0 - \alpha_1 f(\Delta)$. N_0 is introduced to account for the minimal chain-length requirement to have the lipid in a bilayer form; $\alpha_1 f(\Delta)$ is introduced to account for the reduced interaction in

the mismatched region Δ ($0 < \alpha_1 < 1$) with

$$f(\Delta) = \begin{cases} \frac{1}{2}\left(\frac{\Delta^2}{\Delta_{th}} + \Delta_{th}\right), & |\Delta| < \Delta_{th} \\ |\Delta|, & |\Delta| \geq \Delta_{th} \end{cases} \quad (8)$$

Here Δ_{th} represents the threshold value of Δ: when $|\Delta| < \Delta_{th}$, the lipid is assumed to be in a noninterdigitated state and when $|\Delta| \geq \Delta_{th}$, in a partially interdigitated one. In a noninterdigitated state, the mismatched tail of one lipid molecule may randomly collide with another via thermal motions, so that the interaction strength should be proportional to the probability of a two-body collision ($\propto \Delta^2$). In a partially interdigitated state, the interaction strength is assumed to be proportional to $|\Delta|$. Imposing continuous and smooth conditions on f gives Eq. 8. Similarly, C_0 and C_2 are related to excluded-volume interactions and assumed to be proportional to $N - \alpha_2 f(\Delta)$ ($0 < \alpha_2 < 1$). We finally obtain

$$G = H - TS = W_s + U_g + U_{vw} - T(S_g + S_{pk}) \quad (9a)$$

$$W_s = \pi A_0 / r(q) \quad (9b)$$

$$U_g = E_g n_g = E_g (N - 3)\frac{(1 - q)}{2} \quad (9c)$$

$$S_g/R = (N - 1)s_g(q) \quad (9d)$$

$$U_{vw} = -\frac{1}{2}(N - N_0 - \alpha_1 f(\Delta))b(1 - \beta_2 + \beta_2 q^2)r(q)^{5/2} \quad (9e)$$

$$S_{pk}/R = -(N - \alpha_2 f(\Delta))c(1 - \gamma_2 q^2)r(q)^{5/2} \quad (9f)$$

where b is the sublimation energy of a CH_2 monomer; N_0, c, α_1, α_2, β_2, γ_2 are fitting parameters.

Second, similar to the work of Huang and co-workers (Huang et al., 1993b; Li et al., 1994), another structural quantity is defined for the mixed interdigitated (MI) gel phase bilayers. This structural quantity, δ, is the number of unmatched bonds between the length of the longer chain plus its terminal van der Waals radius and the sum of the two shorter chains plus the van der Waals distance between the two chain termini. δ can be expressed as

$$\delta = |\Delta| - (N + 1 - d_{12} - |\Delta|)/2 - d_{vw}/2 \quad (10)$$

where d_{vw} is the van der Waals distance between the two opposing chain termini; δ and d_{vw}, together with Δ, are shown schematically in Fig. 1. Consequently, the Gibbs potential of MI bilayers is similar to that of PI bilayers (Eq. 9), except that Eqs. 9e and 9f are replaced by

$$U_{vw} = -\frac{1}{2}(N - N_0 - \alpha_3|\Delta| - \alpha_4 f(\delta)) \times b(1 - \beta_2 + \beta_2 q^2)r(q)^{5/2} \quad (11e)$$

$$S_{pk}/R = -(N - \alpha_4 f(\delta))c(1 - \gamma_2 q^2)r(q)^{5/2} \quad (11f)$$

where α_3 is a parameter similar to α_1 for PI model, describing the reduced van der Waals interactions in the region $|\Delta|$; α_4 is an MI model-specific parameter for reduced interchain interactions in the unmatched region δ, and f is given by Eq. 8 with Δ being replaced by δ.

Model parameters are obtained by a nonlinear least-square fitting procedure of transition temperature and enthalpy data to Eq. 9 for the PI model or Eq. 11 for the MI model, as described in the Results section. First, however, we will describe the equation of state and Gibbs potential curves for two lipid systems representative of the two kinds of transition processes considered.

Equation of state

Thermodynamic equilibrium requires that at constant temperature the partial derivative of the Gibbs free energy with respect to the order parameter equals zero, i.e.,

$$G_{10}(q, T) = \frac{\partial G(q, T)}{\partial q} = \frac{\partial H(q)}{\partial q} - T\frac{\partial S(q)}{\partial q} = 0 \quad (12)$$

where $G(q, T)$ is given by Eq. 9 or Eq. 11 and Eq. 12 is an *equation of state*, where $q = q(T)$ at constant π. In Fig. 2 the equation of state curve and the Gibbs potential at the transition temperature of C(16)C(16)PC are plotted in *panels A* and *B*, respectively. At low (high) temperature, Eq. 12 has only one solution of a large (small) order parameter, implying that the system is in a gel (fluid) phase. At a temperature near the phase transition temperature, T_m, Eq. 12 has two stable solutions separated by an unstable one, indicating that the system can exist in either phase. At T_m, the two stable solutions have the same Gibbs potential (*panel B*) and the phase transition occurs when the lipid bilayer changes from one state to the other. The dashed line denotes metastable states: between *a* and *b* superheated gel states exist, whereas between *c* and *d* super-cooled fluid states exist. The region between *b* and *c* (*dotted line*) represents unstable states. When the system is at any point, *o*, between *a* and *d*, the system is inhomogeneous, the fraction of lipids in fluid phase is determined by the lever rule: section *ao* divided by section *ad*. The corresponding Gibbs potential that satisfies the global stability condition is the dotted line in *panel B*. This is the pure first-order phase transition picture for PI lipid bilayers.

For lipids with the length of the longer chain about twice that of the shorter one, the bilayer undergoes a MI gel to PI fluid phase transition (McIntosh et al., 1984; Shah et al., 1990; Zhu and Caffrey, 1994), since the bilayer thickness increases upon the gel to fluid transition. To illustrate this kind of phase transition, the equations of state and the Gibbs potentials of the PI and MI models at three temperatures of C(10)C(22)PC are plotted in Fig. 2, *C–F*. In *panel C*, $G_{10}(q, T) = 0$ is shown for possible PI and MI packing arrangements. At temperatures just below T_m (*panel E*), the bilayer is in the MI gel phase since its Gibbs potential is lower than that of the PI fluid phase. At T_m, the MI gel phase and the PI fluid phase have the same Gibbs potential (*panel D*) and the phase transition occurs when the lipid bilayer changes from one phase to the other. At temperatures above T_m (*panel F*), the bilayer exists in the PI fluid phase because its Gibbs potential is lower than that of the MI fluid phase.

For both the PI gel to fluid and the MI gel to PI fluid phase transitions, the transition temperature, T_m, is defined as the temperature at which the gel and fluid phases at equilibrium have the same Gibbs potential, that is, $G_{10}(q_f, T_m) = G_{10}(q_g, T_m) = 0$ and $G(q_f, T_m) = G(q_g, T_m)$, where q_g and q_f are the order parameter values in the gel and fluid states, respectively. The transition enthalpy or latent heat is calculated as $\Delta H_m = H(q_f) - H(q_g)$. When Δ is placed in front of any quantity F, it is viewed as an operator and defined as $\Delta F = F(q_f) - F(q_g)$.

RESULTS

The macroscopic PI model of lipid bilayers (Eq. 9) is used to describe both gel and fluid states and applied to the gel-fluid phase transitions of phosphatidylcholines (PCs) that form PI gel phase bilayers. T_m and ΔH_m values of 39 PCs obtained by differential scanning calorimetry (DSC) experiments are used to fix six adjustable model parameters to achieve a good fit of the model to the data. For PCs

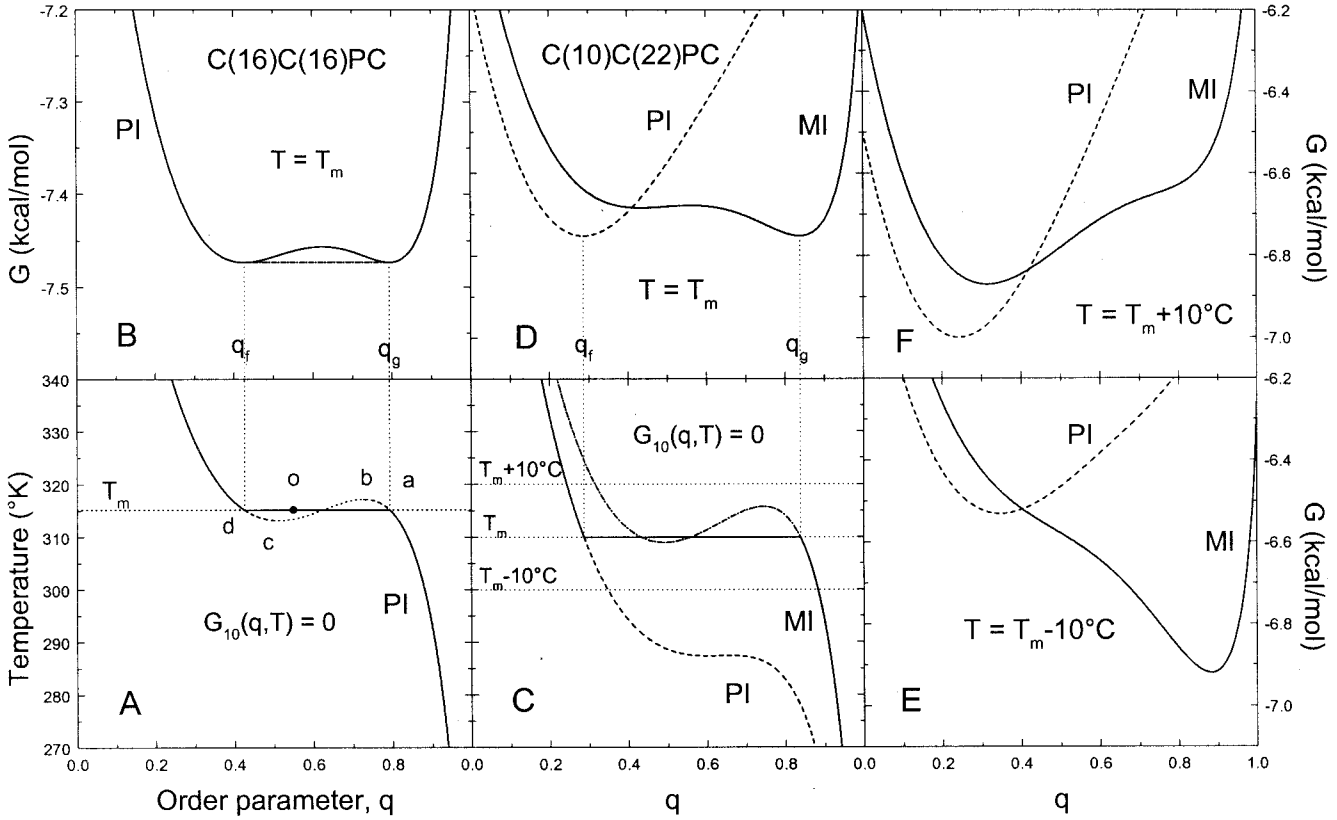

FIGURE 2 Theoretical curves to illustrate the PI gel to fluid phase transition of C(16)C(16)PC (*A* and *B*) and MI gel to PI fluid transition of C(10)C(22)PC (*C–F*). (*A*) The equation of state curve of C(16)C(16)PC. The solid line represents the true equilibrium states. The dashed lines represent meta-stable states, whereas the dotted line represents unstable states. (*B*) The Gibbs potential curve at $T = T_m$, where the two minima have the same values. (*C*) The equation of state curve of C(10)C(22)PC (*solid line*), which consists of MI gel and PI fluid phase curves. (*D–F*) The Gibbs potential curves of possible PI and MI packing structures at T_m, $T_m - 10°C$ and $T_m + 10°C$, respectively.

forming MI gel phase bilayers, the fluid state is described by the PI model (with all parameters fixed) and the gel state by the MI model (Eqs. 9a–d plus Eqs. 11e, f). T_m and ΔH_m values of 56 PCs are used to fix four MI model parameters to achieve a good fit of the MI model to the data. This provides initial confirmation that the proposed model (PI and MI) can accurately represent existing T_m and ΔH_m data. The predicting ability of the model is then tested by its ability to predict T_m and ΔH_m values of 17 other PCs not used in the original fitting procedure. Finally, the model is used to provide macroscopic estimates of other thermodynamic and structural quantities. These estimates provide a further test of the model by comparison with existing experimental or theoretical values and in other cases provide predictions of unknown quantities.

Experimental observations, data analyses, and theoretical considerations yield the estimates of the constant parameters E_g, b, A_0, π, d_{12}, and Δ_{th} of the PI model (Eq. 9); E_g = 0.5 kcal/mol (Nagle, 1980); b = 1838 cal/mol (Salem, 1962). Since the area/chain in the crystal state is ~19.0 Å^2 (Pearson and Pascher, 1979), A_0 = 38.0 Å^2 for PI packing of two chains per headgroup; π = 14.7 dyn/cm (Meraldi and Schlitter, 1981a, b); d_{12} = 1.3 C–C bonds (Marsh, 1992, 1999). It is expected that in order to form a partially interdigitated phase, $|\Delta|$ should be at least equal to the van der Waals distance of chain termini on the opposing leaflets, d_{vw}, so that Δ_{th} = 2.6 C–C bonds (Li et al., 1993). The variable parameters N_0, α_1, α_2, c, β_2, γ_2, are left as empirical constants to be obtained by fitting of the T_m and ΔH_m values of 39 PCs obtained by differential scanning calorimetry (DSC) experiments. These 39 PCs are thought to be in PI gel phase bilayers based on previous work (see references in Table 2). When there are multiple reports for a lipid, an average value is calculated and its associated error estimated. In the case of a single report, that value is used and a maximal error assigned (for T_m, ~1.5°C; for ΔH_m, ~20%). The data with their associated errors are used in a least-square fitting routine (Johnson and Frasier, 1985), where T_m and ΔH_m are calculated numerically. It should be mentioned that in an initial fitting procedure, d_{12} and Δ_{th} were allowed to vary and the values obtained (d_{12} = 1.31 ± 0.10; Δ_{th} = 2.75 ± 0.63) were very close to values cited in the literature. Therefore, the literature values are assumed as noted above.

For PCs forming the MI gel phase bilayers, the fluid state is described by the PI model with parameters values obtained above and the gel state by the MI model (Eqs. 9 a–d plus Eqs. 11 e, f). For the MI model, the constant parameters, E_g, b, d_{12}, A_0, d_{vw}, δ_{th}, c, γ_2, and N_0 are assigned values as follows: E_g, b, and d_{12} are the same as for the PI model; $A_0 = 57.0$ Å^2 for MI packing of three chains per headgroup; $d_{vw} = 2.6$ C–C bonds (Li et al., 1993). Reflecting dynamic effects on chain interactions, δ_{th} is assumed to be 2.6 C–C bonds, the same value as Δ_{th}. Since c and γ_2 are related to the excluded volume interactions and N_0 reflects the minimal chain-length requirement, these three parameters should be insensitive to the chain packing and their values are assumed to be the same as for the PI model obtained above. The variable parameters, π, β_2, α_3, and α_4, are obtained by fitting of T_m and ΔH_m values of 56 PCs that are thought to be in MI gel phase bilayers based on previous work (see references in Table 3). The fitting procedure is similar to that for the PI model, except that q_f is calculated from the PI model while q_g is from the MI model, i.e., $G^{PI}(q_f, T_m) = G^{MI}(q_g, T_m)$. Reflecting the headgroup steric interactions, π is allowed to vary for the three chains per headgroup structure of the MI model; β_2 is also allowed to vary, since the different chain packing structure of the MI model should alter the interchain van der Waals interaction strength; α_3 and α_4 are two MI model specific parameters.

The constant parameters used and the adjustable parameters obtained from the fitting procedures for both PI and MI models are listed in Table 1. The experimental T_m and ΔH_m values of the 39 PCs used in the parameter fitting of the PI model are listed in Table 2, while those of the 56 PCs used in the fitting of MI model are listed in Table 3, along with values obtained from the PI and MI model calculations using Eqs. 9 and 11 with parameter values given in Table 1, respectively. The T_m and ΔH_m data listed in Tables 2 and 3 are plotted as a function of Δ/N in the top and bottom panels of Fig. 3, respectively. The horizontal lines are calculated for the PI and MI models with varying Δ and fixed N (the value is indicated by the number within the figure). The vertical lines are obtained by varying N with fixed Δ for the PI model or fixed δ for the MI model (the Δ or δ value is shown by the numbers within the figure). The agreement between the calculated values and experimental results is excellent for T_m, but less so for ΔH_m. The reason for this larger discrepancy is likely due to the experimental error of ΔH_m being large ($\sim\pm25\%$, Lin et al., 1990), whereas T_m is generally accurate to $\pm1\%$ on the absolute temperature scale. For the 39 PCs in Table 2, the difference between the experimental values and the PI model calculations of T_m are within 1.5°C ($<\pm1\%$ on the absolute temperature scale). For the 56 PCs in Table 3, the difference between the experimental values and the MI model calculations of T_m exceeds 3.0°C ($\sim\pm1\%$) only for C(8)C(19)PC, C(8)C(20)PC, and C(8)C(21)PC. Those ΔH_m data with an associated error bar are plotted and found to agree with the calculated curves within their error bars, except for one very short chain lipid, C(8)C(18)PC (see below).

TABLE 1 Model parameter values for PCs

Parameter	Value		Unit
	PI	MI	
E_g	500	500	cal/mol
A_0	38.0	57.0	Å^2
b	1838	1838	cal/mol/bond
d_{12}	1.3	1.3	C–C bonds
Δ_{th}	2.6	—	C–C bonds
δ_{th}	—	2.6	C–C bonds
d_{vw}	—	2.6	C–C bonds
π	14.7	12.44 ($\pm$0.85)	dyn/cm
N_{min}	9.49 ($\pm$0.10)	9.49	C–C bonds
c	0.934 ($\pm$0.020)	0.934	per bond
γ_2	0.398 ($\pm$0.014)	0.398	—
β_2	0.250 ($\pm$0.022)	0.279 ($\pm$0.006)	—
α_1	0.295 ($\pm$0.013)	—	—
α_2	0.129 ($\pm$0.038)	—	—
α_3	—	0.072 ($\pm$0.005)	—
α_4	—	0.287 ($\pm$0.026)	—

The numbers in parentheses are the confidence intervals for the fitting parameter in the model.

It has been shown above that the calculated values of T_m and ΔH_m agree well with the experimental values. However, since the experimental data were used in the parameter fitting procedures, the comparison was not independent. To test the predicting abilities of the model, we compared the model predictions to experimental observations for lipids whose T_m and ΔH_m values were not used in the parameter fitting procedure. Seventeen lipids have been synthesized and their thermodynamic properties determined in the Huang laboratory. The results are listed in Table 4, along with the model predictions. Some of the data have been published (Huang et al., 1993a, 1994; Li et al., 1994), while the others are unpublished (personal communication). It is evident that the model predictions agree well with experimental observations for all 17 lipids of quite different chain-length and chain-asymmetry variations. These 17 lipids are plotted as diamond symbols in Fig. 3, with 14 belonging to the group of PI gel phase lipids and 2 belonging to the group of MI gel phase lipids. The results for C(14)C(24)PC fall on the boundary distinguishing the PI and MI models. Since the experimental value of ΔH_m of C(14)C(24)PC is not available and both the PI and MI models predict the same T_m, we cannot assign it to either group.

Chain-length dependence

The results of the PI and MI model calculations for some of the lipids shown in Tables 2 and 3 are plotted in Fig. 4 to show the chain-length variations of T_m and ΔH_m. Both PI and MI models predict an almost linear relation for ΔH_m and ΔS_m with N, except at short chain-lengths (Fig. 5),

TABLE 2 Comparison of experimental observations with the PI model calculations of 39 PCs

PC	Δ/N	Δ	T_m^{obs} (°C)	T_m^{cal} (°C)	Difference	ΔH_m^{obs} (kcal/mol)	ΔH_m^{cal} (kcal/mol)	Difference
C(13)C(13)	0.057	1.3	13.7	13.3	−0.4	4.4	4.5	0.1
C(11)C(17)	−0.188	−4.7	13.9	13.4	−0.5	4.0	4.0	0
C(12)C(16)	−0.108	−2.7	21.7	20.6	−1.1	5.7	5.2	−0.5
C(13)C(15)	−0.028	−0.7	25.5	25.2	−0.3	6.0	5.9	−0.1
C(14)C(14)	0.052	1.3	24.0	24.4	0.4	5.8	5.8	0
C(15)C(13)	0.132	3.3	18.8	18.4	−0.4	5.3	4.8	−0.5
C(16)C(12)	0.212	5.3	11.3	11.2	−0.1	4.5	3.5	−1.0
C(11)C(19)	−0.248	−6.7	17.3	17.0	−0.3	4.4	4.0	−0.4
C(12)C(18)	−0.174	−4.7	23.5	23.7	0.2	5.8	5.3	−0.5
C(13)C(17)	−0.100	−2.7	30.5	30.3	−0.2	6.9	6.4	−0.5
C(14)C(16)	−0.026	−0.7	35.0	34.6	−0.4	7.4	7.1	−0.3
C(15)C(15)	0.048	1.3	34.4	33.8	−0.6	7.0	6.9	−0.1
C(16)C(14)	0.122	3.3	28.0	28.3	0.3	6.2	6.1	−0.1
C(17)C(13)	0.196	5.3	21.2	21.7	0.5	5.2	4.9	−0.3
C(12)C(20)	−0.231	−6.7	25.6	26.4	0.8	5.2	5.4	0.2
C(13)C(19)	−0.162	−4.7	32.6	32.5	−0.1	6.7	6.6	−0.1
C(14)C(18)	−0.093	−2.7	38.8	38.6	−0.2	7.9	7.6	−0.3
C(15)C(17)	−0.024	−0.7	41.7	42.6	0.9	10.1	8.2	−1.9
C(16)C(16)	0.045	1.3	41.4	41.9	0.5	8.3	8.1	−0.2
C(17)C(15)	0.114	3.3	37.7	36.8	−0.9	7.4	7.3	−0.1
C(18)C(14)	0.183	5.3	30.5	30.7	0.2	5.9	6.2	0.3
C(13)C(21)	−0.216	−6.7	34.1	34.5	0.4	5.5	6.7	1.2
C(14)C(20)	−0.152	−4.7	39.8	40.2	0.4	7.6	7.7	0.1
C(15)C(19)	−0.087	−2.7	44.8	45.9	1.1	8.7	8.7	0
C(16)C(18)	−0.023	−0.7	49.0	49.6	0.6	9.0	9.3	0.3
C(17)C(17)	0.042	1.3	49.4	48.9	−0.5	9.2	9.2	0
C(18)C(16)	0.106	3.3	44.4	44.2	−0.2	8.1	8.4	0.3
C(19)C(15)	0.171	5.3	39.0	38.5	−0.5	6.4	7.4	1.0
C(20)C(14)	0.235	7.3	33.2	32.8	−0.4	4.7	6.3	1.6
C(15)C(21)	−0.142	−4.7	46.1	46.9	0.8	11.0	8.9	−2.1
C(18)C(18)	0.039	1.3	55.0	55.1	0.1	10.5	10.3	−0.2
C(16)C(22)	−0.134	−4.7	52.8	52.8	0	12.7	10.0	−2.7
C(19)C(19)	0.037	1.3	61.8	60.5	−1.3	10.7	11.4	0.7
C(17)C(23)	−0.127	−4.7	57.9	58.1	0.2	14.0	11.1	−2.9
C(20)C(20)	0.035	1.3	66.4	65.3	−1.1	11.4	12.5	1.1
C(18)C(24)	−0.121	−4.7	62.7	62.8	0.1	15.6	12.2	−3.4
C(21)C(21)	0.033	1.3	71.1	69.6	−1.5	12.2	13.6	1.4
C(22)C(22)	0.032	1.3	74.8	73.5	−1.3	14.9	14.7	−0.2
C(20)C(26)	−0.109	−4.7	70.7	70.8	0.1	18.6	14.4	−4.2

T_m^{obs} and ΔH_m^{obs} are DSC experiment values taken from Huang (1990); Lin et al. (1990, 1991); Wang et al. (1990); Bultmann et al. (1991); Lewis et al. (1987); Mattai et al. (1987); Mabrey and Sturtevant (1978); Chen and Sturtevant (1981); Boggs and Mason (1986); and Stümpel et al. (1983). T_m^{cal} and ΔH_m^{cal} are model calculations of this work.

indicating that with each CH_2 unit increase, the increase of ΔH_m is almost a constant. The T_m plateaus with increasing N and its limiting value is estimated to be 147°C ($N = 10^{100}$ in a model calculation), consistent with the melting temperature of polyethylene (~138–141°C).

For symmetric chain PCs, especially C(14)C(14)PC and C(16)C(16)PC, more information is available. Estimates of ΔU_{vw} have been provided by Nagle and Wilkinson (1978) based upon dilatometry measurements; Δn_g have been estimated directly from Raman spectroscopic studies (Yellin and Levin, 1977; Pink et al., 1980) and indirectly from the ΔU_{vw}. The calculated values are compared with experimental estimates in Table 5. In Fig. 5, the various calculated contributions to the transition enthalpy and entropy, n_g and q at T_m with varying N are shown, along with the limited data in literature for a comparison. The agreement of the PI model predictions with experimental estimates is very good for ΔU_{vw} and quite good for n_g and q. The n_g values estimated by Pink et al. (1980) from Raman spectroscopy with their 10-state model agree with ours in the gel state, but are higher than ours in fluid state. However, ΔU_{vw} of Nagle and Wilkinson (1978) plus ΔU_g computed from Δn_g of Pink et al. (1980) exceeds ΔH_m of DSC measurements. For C(16)C(16)PC at about T_m + 6°C, our model predicts 8.4 *gauche* bonds/lipid, which compares favorably to infrared spectroscopic measured values of 7.8 (Mendelsohn et al., 1989) and 8.4 *gauche* bonds/lipid (Lewis et al., 1994b). The model predicts that ΔU_{vw} makes the major contribution to

TABLE 3 Comparison of experimental observations with the MI model calculations of 56 PCs

PC	Δ/N	δ	T_m^{obs} (°C)	T_m^{cal} (°C)	Difference	ΔH_m^{obs} (kcal/mol)	ΔH_m^{cal} (kcal/mol)	Difference
C(16)C(9)	0.377	0.3	3.6	2.0	−1.6	6.1	7.3	1.2
C(16)C(10)	0.317	−1.7	5.4	5.3	−0.1	6.6	7.6	1.0
C(17)C(9)	0.404	1.3	7.4	7.4	0.0	4.4	7.8	3.4
C(8)C(18)	−0.378	0.4	10.1	8.3	−1.8	7.2	8.0	0.8
C(17)C(10)	0.346	−0.7	13.6	13.5	−0.1	8.4	8.6	0.2
C(18)C(9)	0.429	2.3	11.6	11.1	−0.5	8.2	8.0	−0.2
C(8)C(19)	−0.404	1.4	17.1	13.1	−4.0	10.2	8.4	−1.8
C(9)C(18)	−0.321	−1.6	10.9	11.6	0.7	8.3	8.3	0.0
C(17)C(11)	0.292	−2.7	12.8	13.1	0.3	6.9	8.1	1.2
C(18)C(10)	0.372	0.3	18.8	19.4	0.6	9.0	9.3	0.3
C(19)C(9)	0.452	3.3	14.2	13.4	−0.8	8.3	8.0	−0.3
C(8)C(20)	−0.428	2.4	21.3	16.2	−5.1	12.2	8.6	−3.6
C(9)C(19)	−0.348	−0.6	19.6	19.0	−0.6	11.3	9.2	−2.1
C(10)C(18)	0.268	−3.6	11.4	8.4	−3.0	6.2	6.8	0.6
C(18)C(11)	0.319	−1.7	21.4	21.9	0.5	9.1	9.5	0.4
C(19)C(10)	0.396	1.3	22.7	23.5	0.8	8.3	9.8	1.5
C(8)C(21)	−0.450	3.4	24.3	18.3	−6.0	10.7	8.6	−2.1
C(9)C(20)	−0.373	0.4	24.9	24.2	−0.7	10.9	9.9	−1.0
C(10)C(19)	−0.296	−2.6	19.9	18.9	−1.0	7.1	8.9	1.8
C(18)C(12)	0.270	−3.7	17.6	19.1	1.5	8.4	8.3	−0.1
C(19)C(11)	0.344	−0.7	28.7	28.3	−0.4	10.6	10.5	−0.1
C(20)C(10)	0.419	2.3	25.8	26.1	0.3	10.7	10.0	−0.7
C(9)C(21)	−0.396	1.4	29.3	27.9	−1.4	11.1	10.4	−0.7
C(10)C(20)	−0.322	−1.6	27.2	26.8	−0.4	9.5	10.2	0.7
C(19)C(12)	0.296	−2.7	27.7	27.9	0.2	9.6	10.1	0.5
C(20)C(11)	0.368	0.3	32.8	33.0	0.2	11.1	11.2	0.1
C(21)C(10)	0.439	3.3	27.0	27.7	0.7	11.5	10.0	−1.5
C(9)C(22)	−0.418	2.4	32.0	30.1	−1.9	11.5	10.6	−0.9
C(10)C(21)	−0.346	−0.6	32.7	32.6	−0.1	11.3	11.2	−0.1
C(11)C(20)	−0.275	−3.6	25.7	24.4	−1.3	8.4	9.2	0.8
C(20)C(12)	0.321	−1.7	33.8	34.9	1.1	11.8	11.4	−0.4
C(21)C(11)	0.390	1.3	35.4	36.1	0.7	12.2	11.7	−0.5
C(22)C(10)	0.459	4.3	28.8	29.2	0.4	12.3	10.0	−2.3
C(9)C(23)	−0.438	3.4	33.7	31.5	−2.2	11.4	10.6	−0.8
C(10)C(22)	−0.369	0.4	37.5	36.8	−0.7	12.4	11.9	−0.5
C(11)C(21)	−0.300	−2.6	32.6	32.4	−0.2	9.4	10.8	1.4
C(20)C(13)	0.277	−3.7	30.2	32.5	2.3	11.6	10.5	−1.1
C(21)C(12)	0.343	−0.7	39.6	40.1	0.5	11.8	12.4	0.6
C(22)C(11)	0.410	2.3	37.5	38.1	0.6	12.2	12.0	−0.2
C(10)C(23)	−0.390	1.4	40.0	39.6	−0.4	13.2	12.3	−0.9
C(11)C(22)	−0.323	−1.6	38.6	38.8	0.2	12.6	12.1	−0.5
C(21)C(13)	0.300	−2.7	39.4	39.6	0.2	12.0	12.1	0.1
C(22)C(12)	0.365	0.3	43.0	43.8	0.8	13.3	13.2	−0.1
C(10)C(24)	−0.410	2.4	42.2	41.3	−0.9	13.3	12.6	−0.7
C(11)C(23)	−0.345	−0.6	43.5	43.6	0.1	12.4	13.1	0.7
C(12)C(22)	−0.281	−3.6	37.9	36.7	−1.2	12.2	11.2	−1.0
C(22)C(13)	0.322	−1.7	44.3	45.4	1.1	14.1	13.3	−0.8
C(10)C(25)	−0.428	3.4	43.1	42.3	−0.8	13.1	12.6	−0.5
C(11)C(24)	−0.366	0.4	47.7	46.9	−0.8	13.4	13.8	0.4
C(12)C(23)	−0.303	−2.6	44.0	43.3	−0.7	13.4	12.8	−0.6
C(22)C(14)	0.282	−3.7	41.6	43.3	1.7	12.4	12.5	0.1
C(11)C(25)	−0.385	1.4	49.5	49.2	−0.3	13.7	14.3	0.6
C(12)C(24)	−0.324	−1.6	48.7	48.6	−0.1	13.8	14.0	0.2
C(12)C(26)	−0.363	0.4	55.2	55.3	0.1	14.7	15.7	1.0
C(13)C(25)	−0.306	−2.6	53.3	52.1	−1.2	14.7	14.7	0.0
C(14)C(26)	−0.289	−3.6	55.5	54.9	−0.6	15.1	15.2	0.1

T_m^{obs} and ΔH_m^{obs} are DSC experiment values taken from Huang et al. (1993b); Lin et al. (1991); Lewis et al. (1994a); Xu and Huang (1987); Bultmann et al. (1991); Shah et al. (1990); Mattai et al. (1987); Huang and Mason (1986); Boggs and Mason (1986); and Li et al. (1994). T_m^{cal} and ΔH_m^{cal} are model calculations of this work.

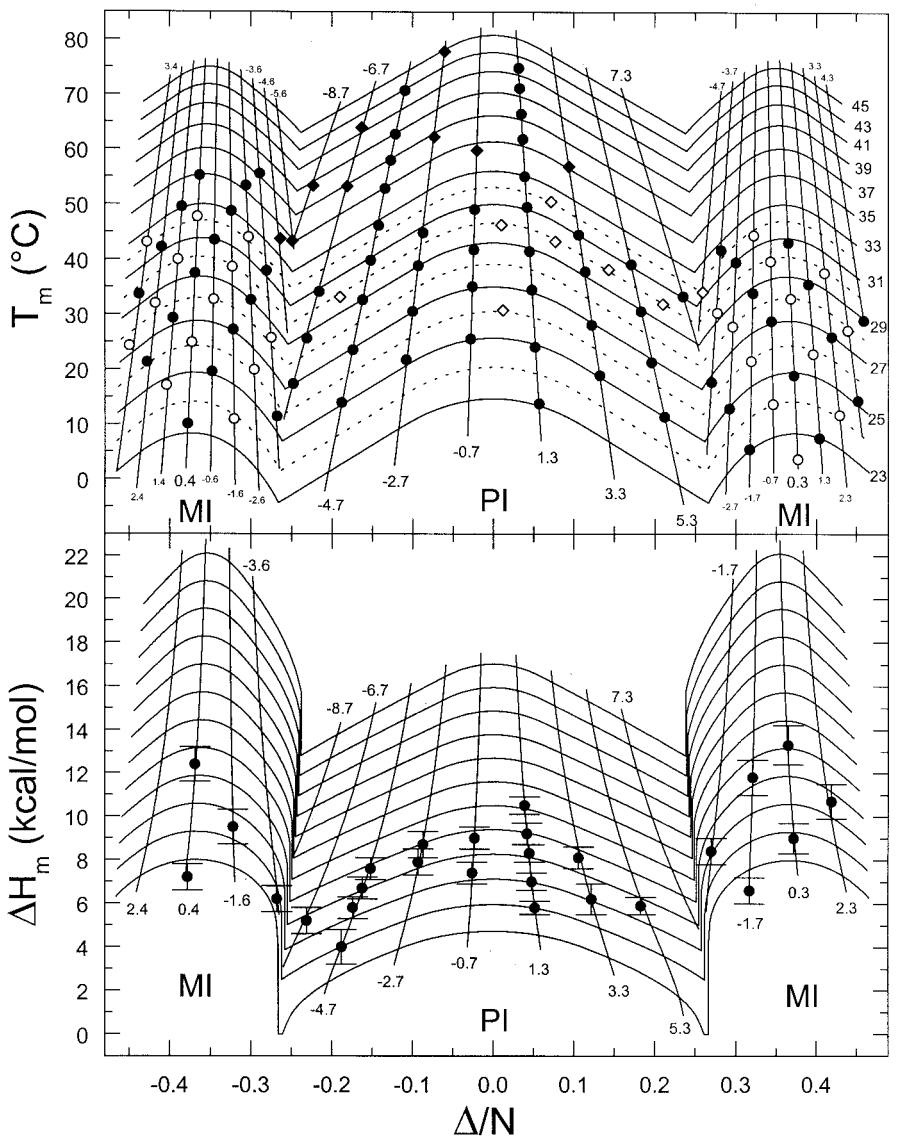

FIGURE 3 T_m (*top*) and ΔH_m (*bottom*) variation with chain-length N and chain-asymmetry Δ. The circles are DSC data listed in Tables 2 and 3. The diamonds are data from Table 4 that have not been used in the model parameter-fitting procedures. The open symbols represent PCs with one chain having an odd number of carbons and the other an even number of carbons. The lines are our model calculations: the horizontal lines are calculated from fixed N (value indicated), whereas the vertical lines are from fixed Δ for the PI model or fixed δ for the MI model (value indicated). The dashed lines are for odd/even PC series.

the transition enthalpy ΔH_m, while the entropy from intrachain *trans-gauche* isomerization, ΔS_g, makes the major contribution to the transition entropy, ΔS_m, as expected.

It is observed (Fig. 5 *D*) from the PI model calculation that, at the phase transition temperature, q increases in the gel state but decreases in the fluid state as N increases. The increased order in the gel phase is apparently due to a stronger van der Waals interaction per bond. To overcome this stronger force requires a higher T_m. The decreased order in the fluid phase is likely the result of the increased thermal motions at elevated T_m, which more than compensate the slightly stronger van der Waals interaction per bond. Therefore, a larger change in the order parameter at its phase transition is observed for a lipid with larger N (see Fig. 5 *D*). This difference is observed in deuterium NMR experiments with C(14)C(14)PC, C(16)C(16)PC, and C(18)C(18)PC (Morrow et al., 1992). The vertex of the curve in Fig. 5 *D* is the critical point predicted by the PI model, where the difference in order parameter between gel phase and fluid phase vanishes. Direct experimental confirmation of this critical point is not feasible because it lies between C(11)C(11)PC and C(10)C(10)PC, whose T_m is far below the freezing point of aqueous dispersions of lipids. It is well known that when a system is close to a critical point, fluctuations of the system become large. Therefore, it is expected from the model that lipid systems with shorter chains will have larger fluctuations. This is consistent with results of the Monte Carlo simulations (Ipsen et al., 1990; Hønger et al., 1996). It should be emphasized that we do not expect the model to provide an accurate description of short chain lipids for which the chain-chain interactions described by the model become less dominant (also recall that Eq. 6 is strictly valid only in the long chain limit). In Fig. 4, *B* and *D,* we see that the enthalpy results of the model calculations

TABLE 4 Comparison of model predictions with experimental observations of 17 PCs

PC	Δ/N	Δ	δ	T_m^{obs} (°C)	T_m^{cal} (°C)	dT_m	ΔH_m^{obs} (kcal/mol)	ΔH_m^{cal} (kcal/mol)	$d\Delta H_m$	Model
C(14)C(15)	0.012	0.3	—	30.7	30.4	−0.3	6.1	6.5	0.4	PI
C(13)C(20)	−0.190	−5.7	—	33.1	33.7	0.6	—	6.7	—	PI
C(16)C(17)	0.010	0.3	—	46.2	46.5	0.3	8.4	8.8	0.4	PI
C(17)C(16)	0.077	2.3	—	43.2	43.6	0.4	7.8	8.4	0.6	PI
C(18)C(15)	0.143	4.3	—	38.1	37.8	−0.3	7.5	7.4	−0.1	PI
C(19)C(14)	0.210	6.3	—	31.8	31.9	0.1	6.3	6.3	0.0	PI
C(18)C(17)	0.072	2.3	—	50.4	50.3	−0.1	9.1	9.5	0.4	PI
C(18)C(20)	−0.020	−0.7	—	59.7	61.1	1.4	10.7	11.6	0.9	PI
C(20)C(18)	0.094	3.3	—	56.8	56.4	−0.4	10.1	10.7	0.6	PI
C(16)C(24)	−0.181	−6.7	—	53.2	53.5	0.3	—	10.2	—	PI
C(18)C(22)	−0.073	−2.7	—	62.2	62.8	0.6	11.2	12.1	0.9	PI
C(16)C(26)	−0.223	−8.7	—	53.3	54.0	0.7	—	10.4	—	PI
C(18)C(26)	−0.163	−6.7	—	63.9	62.9	−1.0	13.1	12.5	−0.6	PI
C(22)C(26)	−0.060	−2.7	—	77.8	78.2	0.4	15.8	16.4	0.6	PI
C(14)C(24)	−0.249	−8.7	−5.6	43.3	43.5	0.2	—	—	—	Unknown
C(21)C(14)	0.259	—	−4.7	34.0	36.5	2.5	—	10.5	—	MI
C(13)C(23)	−0.264	—	−4.6	43.7	40.4	−3.3	13.8	11.4	−2.4	MI

Some experimental data are from Huang et al. (1993b, 1994) and Li et al. (1994), the others are the unpublished data from the Huang laboratory. The model calculations are this work. $dT_m = T_m^{cal} - T_m^{obs}$; $d\Delta H_m = \Delta H_m^{cal} - \Delta H_m^{obs}$.

tend to deviate from experimental observations at short chain-lengths.

Chain-asymmetry dependence

In Fig. 6, the T_m of C(15)C(15)PC series ($N = 27$) and C(16)C(16)PC series ($N = 29$) and ΔH_m of C(15)C(15)PC series are plotted in the top and bottom panels, respectively. Variation of T_m with chain-asymmetry of these two series and some others have been extensively studied by Huang and co-workers (Lin et al., 1991; Huang et al., 1993a). Recall that Δ is a measure of mismatched bonds between *sn*-1 and *sn*-2 chains and δ is a measure of the unmatched bonds in the MI packing structure. For a lipid series with constant N, as $|\Delta|$ increases from $|\Delta| = 0$, both T_m and ΔH_m decrease due to decreased van der Waals interactions in the mismatched region in the gel state. As $|\Delta|$ increases beyond a certain point, lipids such as C(18)C(12)PC prefer the MI gel phase because of its lower Gibbs potential. The T_m and ΔH_m begin to increase due to favored van der Waals interactions in the MI gel phase until the maximal values are reached at $|\delta| = 0$. It is noted that there is a large discontinuous change of ΔH_m at the boundary distinguishing PI and MI packing (indicated by the dotted lines in the bottom panel of Fig. 6), while T_m is continuous across this boundary.

Based on their extensive synthetic and DSC studies, and molecular mechanics study of the C(14)C(14)PC series, Huang and co-workers suggested that lipids with $\Delta C/CL < 0.41$ prefer the PI gel phase, while those with $\Delta C/CL > 0.41$ prefer the MI gel phase (Lin et al., 1991; Li et al., 1994), where $\Delta C = |\Delta|$, and CL is the effective length of the longer chain. The $|\Delta|/N$ boundary value between PI and MI packing can be estimated by our model in terms of the two structural quantities, Δ and N. The results from C(13)C(13)PC series to C(26)C(26)PC series are listed in Table 6, along with the equivalent $\Delta C/CL$ values and the discontinuous changes in ΔH_m. Generally speaking, when $|\Delta|/N$ is less than the boundary value, the lipid is anticipated to exist in the PI gel phase and when $|\Delta|/N$ is greater than the boundary value, in the MI gel phase. But when $|\Delta|/N$ value of a lipid is very close to the corresponding boundary value, its gel phase structure cannot be predicted by the values of Δ and N alone. However, comparison of the experimentally measured ΔH_m with the model values allows such a distinction to be made. For an illustration, see C(11)C(19)PC and C(18)C(12)PC in Fig. 6. Both lipids lie close to the boundary with their T_m values close to each other and model predictions. However, their ΔH_m values differ by ~4 kcal/mol. Based upon the model calculations, one would anticipate that C(11)C(19)PC is in the PI gel phase, while C(18)C(12)PC is in the MI gel phase. It is noted that the boundary value decreases monotonously with increasing N, while the change of ΔH_m initially increases and then decreases slightly, remaining essentially constant.

For the C(16)C(16)PC series ($N = 29$), the various contributions to the excess enthalpy and entropy, n_g and q, have been calculated at the transition temperature and are shown in Fig. 7, along with limited data from the literature for a comparison. It is apparent that both the PI and MI model calculations agree well with the limited experimental measurements available. Both the PI and MI models predict that ΔU_{vw} makes the dominate contribution to ΔH_m, while ΔS_g makes the dominate contribution to ΔS_m. As $|\Delta|$ increases from zero, q decreases in the gel phase and increases in the fluid phase at the T_m. As $|\Delta|$ increases further, q increases discontinuously in the gel phase as the lipids shift from PI

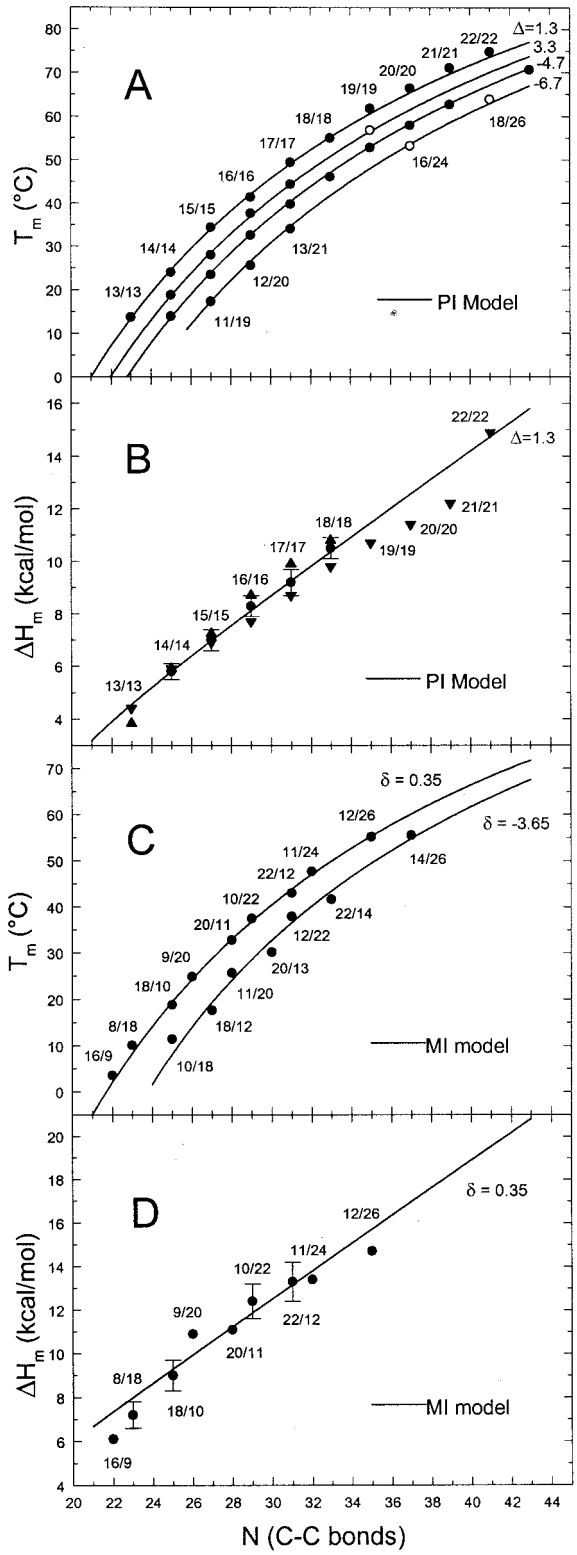

FIGURE 4 T_m and ΔH_m variation with chain-length N of PI series (*A* and *B*) and MI series (*C* and *D*). The symbols are experimental observations from DSC: ●, the average value in the original data set listed in Tables 2 and 3; ○, not used in the fitting procedure (in Table 4); ▲, Ichimori et al. (1998); ▼, Lewis et al. (1987). The lines are model calculations. A short notation is used for C(X)C(Y)PC as X/Y, which is also used in Figs. 5–7.

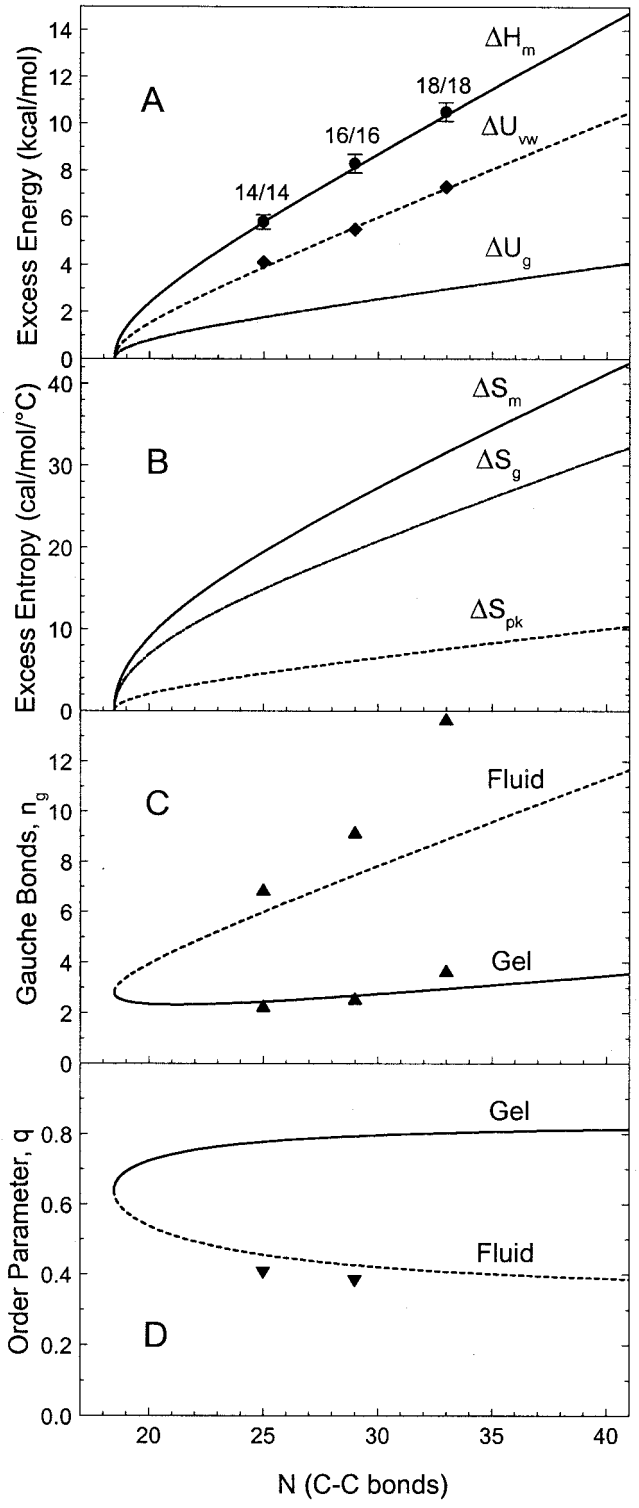

FIGURE 5 Model calculations of symmetric PC series with varying chain-length N at T_m: *A*, various contributions to the excess enthalpy; *B*, contributions to the excess entropy; *C*, the number of *gauche* bonds; and *D*, the order parameter. For comparison, the experimental data of ΔH_m, ΔU_{vw}, n_g, and q (listed in Tables 2 or 5) are included as symbols: ●, DSC average values; ◆, dilatometry of Nagle and Wilkinson (1978); ▲, Raman spectroscopy of Pink et al. (1980); ▼, deuterium NMR of Seelig and Seelig (1974) and Marsh et al. (1983).

TABLE 5 Comparison of experiments and theoretical models on transition changes of *gauche* bonds, van der Waals energy, and order parameter of C(14)C(14)PC, C(16)C(16)PC, and C(18)C(18)PC at transition temperature T_m

	Δn_g				ΔU_{vw} (kcal/mol)			q_f		
PC	Experiment		Model		Experiment	Model		Experiment	Model	
C(14)C(14)	4.6*	3.2†	3.5‡	—§	4.1†	3.9‡	—§	0.410¶	0.455‡	—§
C(16)C(16)	6.6*	5.6†	4.8‡	4.9§	5.5†	5.6‡	5.6§	0.386¶	0.426‡	0.39§
C(18)C(18)	10.0*	5.6†	5.9‡	—§	7.3†	7.2‡	—§	—¶	0.408‡	—§

* Source: Pink et al., 1980.
† Source: Nagle and Wilkinson, 1978.
‡ Source: This work.
§ Source: Meraldi and Schlitter, 1981a, b.
¶ Source: Seelig and Seelig, 1974; Marsh et al., 1983; Marsh, 1990.

to MI packing, but decreases continuously in the fluid phase, resulting in a larger change of q. This discontinuous change of q is due to the structural change from PI to MI packing in the gel phase, resulting in a 2.7 kcal/mol discontinuous change in ΔH_m. With further increase of $|\Delta|/N$ until $|\delta| = 0$, q decreases rapidly in the fluid phase due to the increase of T_m.

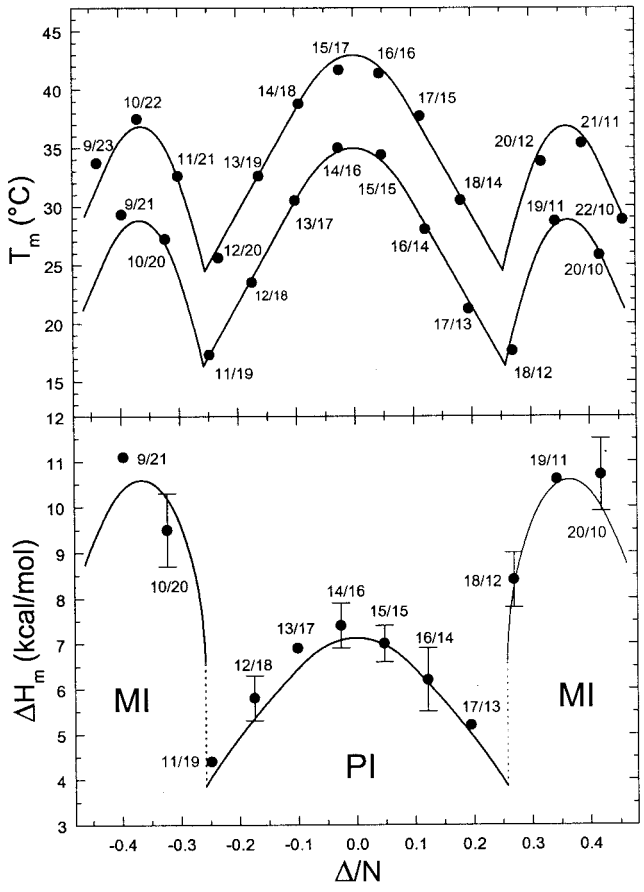

FIGURE 6 Chain-asymmetry dependence of T_m (*top*) of C(15)C(15)PC and C(16)C(16)PC series and ΔH_m (*bottom*) of C(15)C(15)PC series. ● is the DSC average value listed in Tables 2 or 3, mainly from Huang and co-workers (Lin et al., 1991; Bultmann et al., 1991; Huang et al., 1993b). The lines are model calculations from this work.

Temperature effect on chain order and *gauche* conformers

Above T_m, the chain order decreases and *gauche* conformers increase with increasing temperature due to increased thermal motions. The chain order is usually studied by deuterium NMR (Seelig and Seelig, 1974). Recently, *gauche* conformers have been studied by FTIR (Mendelsohn et al., 1989; Lewis et al., 1994b) and by NMR with the *kink* and *jog* model (Douliez et al., 1995, 1996). Some results are listed in Table 7 and compared to our results. Douliez et al. studied separately the *sn*-1 and *sn*-2 chains of C(14)C(14)PC with and without 30% cholesterol at various temperatures. Since the first bond of the *sn*-2 chain is approximately parallel to the bilayer surface, we feel that the results of the *sn*-1 chain represent the bilayer interior more accurately and is thus used for comparison in Table 7. The difference between experimental and calculated values are within ±11% for the order parameter and ±4% for the total *gauche* conformers.

TABLE 6 Variation of boundary values of $|\Delta|/N$, $\Delta C/CL$, and the changes in ΔH_m with the chain-length for lipids from C(13)C(13)PC series (N = 23) to C(26)C(26)PC series (N = 49) predicted by the model

N	$\lvert\Delta\rvert/N$	$\Delta C/CL$	$\Delta\Delta H_m$ (kcal/mol)
23	0.266	0.425	—
25	0.262	0.419	2.91
27	0.258	0.414	2.76
29	0.255	0.409	2.70
31	0.252	0.405	2.68
33	0.249	0.402	2.70
35	0.247	0.399	2.73
37	0.245	0.396	2.76
39	0.243	0.393	2.80
41	0.241	0.391	2.85
43	0.239	0.389	2.89
45	0.238	0.387	2.95
47	0.237	0.385	3.00
49	0.236	0.383	3.05

$\Delta\Delta H_m = \Delta H_m^{MI} - \Delta H_m^{PI}$ at the boundary.

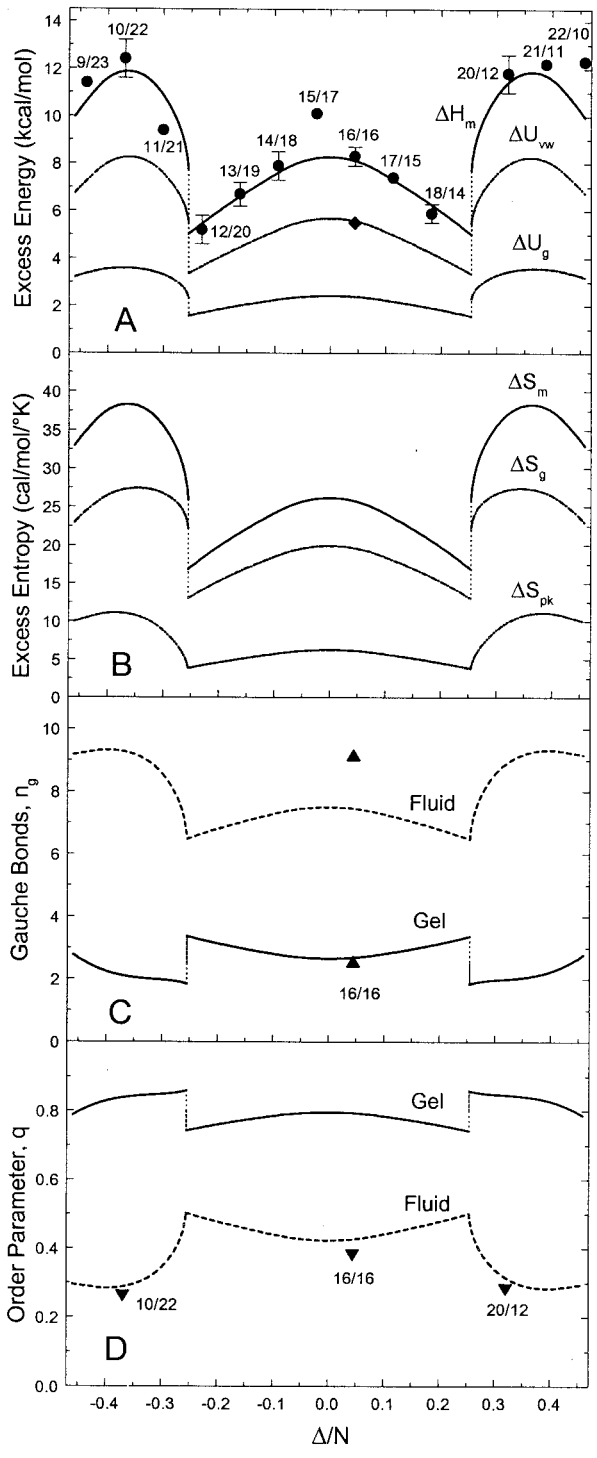

FIGURE 7 Model calculation of C(16)C(16)PC series with varying chain-asymmetry Δ at T_m: *A*, various contributions to excess enthalpy; *B*, contributions to excess entropy; *C*, the number of *gauche* bonds; and *D*, the order parameter. For comparison, the experimental data of ΔH_m, ΔU_{vw}, n_g, and q (listed in Tables 2, 3, 5, or 7) are included as symbols: ●, DSC data; ◆, dilatometry of Nagle and Wilkinson (1978); ▲, Raman spectroscopy of Pink et al. (1980); ▼, deuterium NMR of Seelig and Seelig (1974) and Lewis et al. (1994b). The DSC data with an error bar are averages and those without an error bar are from a single experimental report, and tend to have large errors.

DISCUSSION

In this work, a macroscopic representation for the gel-fluid transition is proposed for mixed-chain saturated PCs. The model parameters are obtained by fitting T_m and ΔH_m values of DSC measurements to the model. The proposed model (both PI and MI) indicates that interchain van der Waals interaction energy makes the major contribution to ΔH_m, and the entropy from intrachain *trans-gauche* isomerization makes the major contribution to ΔS_m, as expected (Figs. 5 and 7). This is consistent with the general consensus that the lipid bilayer gel to fluid phase transition is mainly entropy-driven due to *trans-gauche* isomerization at the expense of van der Waals interactions (Nagle, 1980). The excellent agreement between experimental and predicted values of T_m and ΔH_m indicates that the model provides an accurate description of the thermodynamic changes associated with lipid bilayer phase transitions. The model is further justified by the good agreement between the model estimates and experimental observations of ΔU_{vw}, n_g, and q using various techniques. It is noted that no experimental information relating ΔU_{vw}, n_g, and q has been used in the fitting procedure.

Among the six adjustable parameters of the PI model listed in Table 1, c, β_2, and γ_2 are highly correlated (the absolute values of their cross-correlation coefficients are 0.99). However, if c is fixed, the cross-correlation between β_2 and γ_2 is significantly reduced. The physical meanings of β_2 and γ_2 are not very clear, but are thought to reflect chain conformations (Meraldi and Schlitter, 1981a, b). The physical meaning of c may be that it is related to the maximal excluded volume interaction in the high temperature limit ($q \rightarrow 0$).

In our calculation of the area/lipid, Eq. 4 tends to underestimate A, since it overestimates $\langle\cos\theta\rangle$. The conventional relationship (Schindler and Seelig, 1975; Nagle, 1993) can be written in our notation as

$$r(q) = (1 + q)/2 \tag{13}$$

Equations 13 and 4 have been investigated with molecular dynamics simulation by Berger et al. (1997) and by Petrache et al. (1999), who derived an alternative formula, which in our notation is

$$r(q) = \frac{1}{2}\left(1 + \sqrt{\frac{4q - 1}{3}}\right) \tag{14}$$

When Eqs. 13 and 14 are used instead of Eq. 4 in the PI model to fit the 39 PC data listed in Table 2, all fitting parameters obtained, except β_2 and γ_2, fall within the confidence intervals listed in Table 1. The calculated results are essentially identical to the calculated values listed in Table 2 (within ±0.1°C for T_m and ±0.1 kcal/mol for ΔH_m) with similar statistics, indicating Eqs. 4, 13, and 14 all work equivalently well in the model. The reasons may be that we

TABLE 7 Comparisons of our calculations with experimental values of the order parameter and total *gauche* conformers per molecule

Lipid	T (°C)	q (+ 30% cholesterol)	n_g (+ 30% cholesterol)	q Experiment	q Model	n_g Experiment	n_g Model
C(14)C(14)PC (*sn*-1 chain)	20	0.775	2.1				
	25	0.741	2.4	0.404	0.442	6.2	6.1
	30	0.706	2.8	0.346	0.371	7.1	6.9
	35	0.676	3.2	0.315	0.328	7.6	7.4
	40	0.645	3.6	0.291	0.296	8.0	7.8
	45	0.621	3.9	0.276	0.270	8.2	8.0
	50	0.601	4.1	0.262	0.247	8.3	8.3
	55			0.246	0.228	8.5	8.5
	60			0.235	0.210	8.7	8.7
C(16)C(16)PC	T_m + 6			0.354	0.351	8.4	8.4
C(20)C(12)PC	T_m + 6			0.284	0.282	9.0	9.3
C(10)C(22)PC	T_m + 6			0.268	0.259	9.4	9.6

The experimental data of C(14)C(14)PC are estimated from Douliez et al. (1996) and the rest from Lewis et al. (1994b), except that q of C(16)C(16)PC is from Seelig and Seelig (1974). The calculated values are from this work.

only use average quantities (for which Eqs. 13 and 14 give similar values due to compensations of errors as shown by Petrache et al., 1999) and that the adjustable parameters, β_2 and γ_2, are able to accommodate any differences. However, all three equations result in essentially the same estimates of the other fitting parameters that have clearer physical meaning.

In relating f_g to q, we used the two extreme conditions ($q = 0, 1$) to propose Eq. 5. There are many other relationships that also satisfy the two extreme conditions, for example,

$$f_g(q) = (1 - q^{\alpha})/2 \tag{15}$$

with α in the interval $(0, +\infty)$. Equation 15 reduces to Eq. 5 for $\alpha = 1$. When Eq. 15 with $\alpha = 1/2$ or 2 is used to replace Eq. 5 in the PI model to fit the 39 PC data listed in Table 2, no adequate fitting parameters can be found to describe the main transitions (no sharp transition is produced for any lipid). Only when α is very close to 1 does the model work reasonably well, indicating Eq. 5 may be a very good approximation. To further test the validity of Eq. 5, experimental data listed in Table 7 are plotted in Fig. 8, where f_g is n_g divided by the total number of carbon bonds. The data of C(14)C(14)PC with 30% cholesterol are also included, since Eq. 5 is proposed as a general relationship between q and f_g regardless of lipid bilayer phases or experimental conditions. The experimental data indicate an almost linear relationship between q and f_g, in accordance with Eq. 5. The experimental data are somewhat lower than the straight line of Eq. 5, but can be accommodated by adding ~0.4 *gauche* bonds/chain. Experimental values of the number of *gauche* conformers were obtained using assumptions that only certain *gauche* conformations exist, thus these values can be underestimates of the actual values.

Equation 8 is an empirical equation to phenomenologically describe the interchain interaction dependence on chain mismatch. The functional form seems to be successful in accounting for the chain-asymmetry dependence of transition properties (see Figs. 3, 6, and 7). For the PI model, the values of α_1 and α_2 obtained from fitting are 0.295 and 0.129, respectively, meaning that the interchain van der Waals and excluded volume interaction strengths are reduced by ~30% and 13%, respectively, in the mismatched region compared to the well-matched region of the chain pairs. The value of α_3 of the MI model is ~0.07 compared to 0.295 for α_1 of the PI model, indicating that interchain van der Waals interactions of the MI packing mode are much stronger than those of PI packing. This is consistent with the observation that ΔH_m of the MI gel to PI fluid transition is much larger than that of the PI gel to fluid phase transition (compare Tables 2 and 3, also see Figs. 3, 4, 6, and 7 for lipids with the same N). We found it necessary to

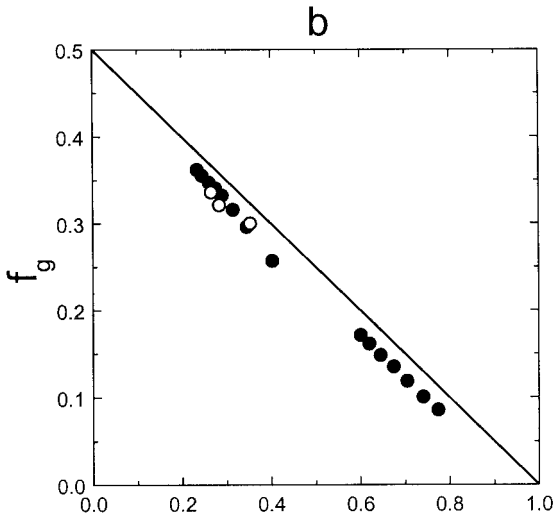

FIGURE 8 Comparison of the proposed Eq. 5 and experimental data listed in Table 7 to show the relationship between the fraction of *gauche* conformers and the order parameter. The line is calculated from Eq. 5. The symbols are: ●, Douliez et al. (1996); ○, Lewis et al. (1994b).

lower the value of π from 14.7 dyn/cm for PI model to ~12.4 dyn/cm for the MI model. This is consistent with the fact that MI packing is three acyl chains per headgroup, so that the headgroup steric interactions should be reduced compared to PI packing of two chains per headgroup. The fact that both PI and MI models share a number of common empirical constants (E_g, b, d_{12}, N_0, c, and γ_2) indicates that the proposed model provides a satisfactory general description of the gel-fluid phase transitions of saturated lipid bilayers.

Our calculations indicate that the change in q for the MI gel to PI fluid transitions at the T_m is larger than the change in q for the PI gel to fluid transitions, primarily because the MI bilayer is more ordered in the gel phase, thus resulting in a much larger ΔH_m. However, T_m is continuous across the PI and MI boundary as a function of $|\Delta|/N$ and remains the same order of magnitude for both transitions. Both T_m and ΔH_m reach maximal values at $\Delta = 0$ for the PI gel-fluid transition and at $\delta = 0$ for the MI gel to PI fluid transition, but minimal values at the boundary between the PI and MI lipid classes, where the mismatch ($|\Delta|$ or $|\delta|$) is largest. The $|\Delta|/N$ boundary value that separates PI and MI packing predicted by the model is ~0.25, indicating that when the effective chain mismatch exceeds about a quarter of the total chain length, lipids prefer the MI gel phase packing structure. This value corresponds to $\sim\Delta C/CL = 0.41$, a result in accordance with that of Huang and co-workers (Lin et al., 1991; Li et al., 1993). However, our calculations reveal that this boundary value is not a constant as implied (Lin et al., 1991), but varies with total effective chain-length, N.

In summary, a macroscopic model has been developed and applied to two classes of mixed-chain saturated PCs. The basic postulate is that lipid bilayer gel-fluid phase transitions can be characterized by a single-order parameter. Incorporation of chain-length and chain-asymmetry dependence into the Gibbs potential of lipid bilayers in this model describes all lipids in one class with one equation and its associated parameters. The input into the model is the experimental results of T_m and ΔH_m of 39 lipids for PI and 56 lipids for the MI model, and the output (predictions) include not only T_m and ΔH_m, but van der Waals interaction energy, bond rotational entropy, packing entropy (excluded volume interaction), number of *gauche* bonds, and the order parameter. The model shows excellent agreement with existing experimental measurements obtained using various techniques and appears to have very good predicting power. The model can also serve as a transformation of thermodynamic results (T_m, ΔH_m) into structural information (n_g, q) and provide access to information on quantities not easily accessible from experiment (U_{vw}, S_g, S_{pk}).

It may be mentioned that the calculated data presented so far are only part of all possible lipids (427 from the C(13)C(13)PC series to the C(26)C(26)PC series) in two general classes. Although the model developed here is for only saturated PCs, only the fitting parameters are specific to them. It is straightforward to apply the model (Eqs. 9 and 11) with adjustment of only a few parameter values to other saturated lipids such as phosphatidylethanolamines (PEs), for which there also is a relatively abundant experimental information base (Huang et al., 1994). It is also expected that with some modifications, the model can be applied to PCs and PEs with a saturated *sn*-1 chain and one double bond on an *sn*-2 chain (Huang et al., 1996). In addition, it is expected that with reliable estimates of the Gibbs potential using this model, phase diagrams of binary mixtures can be predicted following Priest (1980) and Sugár and Monticelli (1985).

The application of this approach to more complex mixtures could lead to a better general understanding of the phase behavior of bilayers in general. This will be particularly true if used in conjunction with other experimental and theoretical tools such as x-ray diffraction, NMR, Monte Carlo simulations, and molecular dynamics calculations. Mixing (demixing) behavior of complex lipids can play an important role in protein localization or colocalization on and within the membrane leading to altered reaction rates, diffusion, and protein association (Thompson et al., 1995; Dibble et al., 1996; Hinderliter et al., 1997; Gil et al., 1998; Sabra and Mouritsen, 1998). For example, to what extent is "raft" formation in the plasma membrane (Simons and Ikonen, 1997) modulated by the thermodynamics of lipid-lipid interactions? Knowledge of the magnitude of such interactions is crucial to the development of an understanding of modulation of membrane function by membrane composition and structure.

We thank Dr. Ching-hsien Huang for his encouragement and kind provision of his unpublished DSC data, and Dr. István P. Sugár and Dr. Thomas E. Thompson for their critical readings of the manuscript. We thank one reviewer whose detailed comments helped to enhance the quality of this paper.

This work was supported by National Science Foundation Grant MCB-9632095 and National Institutes of Health Grant GM59205.

REFERENCES

Berger, O., O. Edholm, and F. Jähnig. 1997. Molecular dynamics simulations of a fluid bilayer of dipalmitoylphosphatidylcholine at full hydration, constant pressure, and constant temperature. *Biophys. J.* 72: 2002–2013.

Biltonen, R. L. 1990. A statistical-thermodynamic view of cooperative structural changes in phospholipid bilayer membranes: their potential role in biological function. *J. Chem. Thermodyn.* 22:1–19.

Boggs, J. M., and J. T. Mason. 1986. Calorimetric and fatty acid spin label study of subgel and interdigitated gel phases formed by asymmetric phosphatidylcholines. *Biochim. Biophys. Acta.* 863:231–242.

Bultmann, T., H.-N. Lin, Z.-Q. Wang, and C.-H. Huang. 1991. Thermotropic and mixing behavior of mixed-chain phosphatidylcholines with molecular weights identical to that of L-α-dipalmitoylphosphatidylcholine. *Biochemistry.* 30:7194–7202.

Caillé, A., D. Pink, F. de Verteuil, and M. J. Zuckermann. 1980. Theoretical models for quasi-two-dimensional mesomorphic monolayers and membrane bilayers. *Can. J. Phys.* 58:581–611.

Cevc, G., and D. Marsh. 1987. Phospholipid Bilayers: Physical Principles and Models. John Wiley & Sons, New York.

Chen, S. C., and J. M. Sturtevant. 1981. Thermotropic behavior of bilayers formed from mixed-chain phosphatidylcholines. *Biochemistry.* 20: 713–718.

Cotter, M. A. 1977. Hard spherocylinders in an anisotropic mean field: a simple model for a nematic liquid crystal. *J. Chem. Phys.* 66: 1098–1106.

de Gennes, P. G. 1971. Short range order effects in the isotropic phase of nematics and cholesterics. *Mol. Cryst. Liq. Cryst.* 12:193–214.

Dibble, A. R. G., A. K. Hinderliter, J. J. Sando, and R. L. Biltonen. 1996. Lipid lateral heterogeneity in phosphatidylcholine/phosphatidylserine/diacylglycerol vesicles and its influence on protein kinase C activation. *Biophys. J.* 71:1877–1890.

Doniach, S. 1978. Thermodynamic fluctuations in phospholipid bilayers. *J. Chem. Phys.* 68:4912–4916.

Douliez, J.-P., A. Léonard, and E. Dufourc. 1995. Restatement of order parameters in biomembranes: calculation of C–C bond order parameters from C–D quadrupolar splittings. *Biophys. J.* 68:1727–1739.

Douliez, J.-P., A. Léonard, and E. Dufourc. 1996. Conformational order of DMPC sn-1 versus sn-2 chains and membrane thickness: an approach to molecular protrusion by solid state ^{2}H-NMR and neutron diffraction. *J. Phys. Chem.* 100:18450–18457.

Flory, P. J. 1969. Statistical Mechanics of Chain Molecules. Interscience, New York.

Gelbart, W. M., and B. A. Baron. 1977. Generalized van der Waals theory of the isotropic-nematic phase transition. *J. Chem. Phys.* 66:207–213.

Gil, T., J. H. Ipsen, O. G. Mouritsen, M. C. Sabra, M. M. Sperotto, and M. J. Zuckermann. 1998. Theoretical analysis of protein organization in lipid membranes. *Biochim. Biophys. Acta.* 1376:245–266.

Halladay, H. N., R. E. Stark, S. Ali, and R. Bittman. 1990. Magic-angle spinning NMR studies of molecular organization in multibilayers formed by 1-octadecanoyl-2-decanoyl-sn-glycerol-3-phosphocholine. *Biophys. J.* 58:1449–1461.

Hinderliter, A. K., P. F. F. Almeida, R. L. Biltonen, and C. E. Creutz. 1998. Membrane domain formation by calcium-dependent, lipid-binding proteins: insights from the C2 motif. *Biochim. Biophys. Acta.* 1448: 227–235.

Hinderliter, A. K., A. R. G. Dibble, R. L. Biltonen, and J. J. Sando. 1997. Activation of protein kinase C by coexisting diacylglycerol-enriched and diacylglycerol-poor lipid domains. *Biochemistry.* 36:6141–6148.

Hønger T., K. Jørgensen, R. L. Biltonen, and O. G. Mouritsen. 1996. Systematic relationship between phospholipase A_2 activity and dynamic lipid bilayer microheterogeneity. *Biochemistry.* 35:9003–9006.

Huang, C. 1990. Mixed-chain phospholipids and interdigitated bilayer systems. *Klin. Wochenschr.* 68:149–165.

Huang, C. 1991. Empirical estimation of the gel to liquid-crystalline phase transition temperatures for fully hydrated saturated phosphatidylcholines. *Biochemistry.* 30:26–30.

Huang, C., and S. Li. 1999. Calorimetric and molecular mechanics studies of the thermotropic phase behavior of membrane phospholipids. *Biochim. Biophys. Acta.* 1422:273–307.

Huang, C., S. Li, H.-N. Lin, and G. Wang. 1996. On the bilayer phase transition temperatures for monoenoic phosphatidylcholines and phosphatidylethanolamines and the interconversion between them. *Arch. Biochem. Biophys.* 334:135–142.

Huang, C., S. Li, Z.-Q. Wang, and H.-N. Lin. 1993a. Dependence of the bilayer phase transition temperatures on the structural parameters of phosphatidylcholines. *Lipids.* 28:365–370.

Huang, C., and J. T. Mason. 1986. Structure and properties of mixed-chain phospholipid assemblies. *Biochim. Biophys. Acta.* 864:423–470.

Huang, C., J. T. Mason, and I. W. Levin. 1983. Raman spectroscopic studies of saturated mixed-chain phosphatidylcholine multilamellar dispersions. *Biochemistry.* 22:2775–2780.

Huang, J., J. E. Swanson, A. R. G. Dibble, A. K. Hinderliter, and G. W. Feigenson. 1993c. Nonideal mixing of phosphatidylserine and phosphatidylcholine in the fluid lamellar phase. *Biophys. J.* 64:413–425.

Huang, C., Z.-Q. Wang, H.-N. Lin, and E. E. Brumbaugh. 1993b. Calorimetric studies of fully hydrated phosphatidylcholines with highly asymmetric acyl chains. *Biochim. Biophys. Acta.* 1145:293–310.

Huang, C., Z.-Q. Wang, H.-N. Lin, E. E. Brumbaugh, and S. Li. 1994. Interconversion of bilayer phase transition temperatures between phosphatidylethanolamines and phosphatidylcholines. *Biochim. Biophys. Acta.* 1189:7–12.

Hui, S. W., J. T. Mason, and C. H. Huang. 1984. Acyl chain interdigitation in saturated mixed-chain phosphatidylcholine bilayer dispersions. *Biochemistry.* 23:5570–5577.

Ichimori, H., T. Hata, H. Matsuki, and S. Kaneshina. 1998. Barotropic phase transitions and pressure-induced interdigitation on bilayer membranes of phospholipids with varying acyl chain lengths. *Biochim. Biophys. Acta.* 1414:165–174.

Ipsen, J. H., K. Jørgensen, and O. G. Mouritsen. 1990. Density fluctuations in saturated phospholipid bilayers increase as the acyl-chain length decreases. *Biophys. J.* 58:1099–1107.

Jähnig, F. 1981. Critical effects from lipid-protein interaction in membranes. I. Theoretical description. *Biophys. J.* 36:329–345.

Jerala, R., P. F. F. Almeida, and R. L. Biltonen. 1996. Simulation of the gel-fluid transition in a membrane composed of lipids with two connected acyl chains: application of a dimer-move step. *Biophys. J.* 71: 609–615.

Johnson, M. L., and S. G. Frasier. 1985. Nonlinear least-square analysis. *Methods Enzymol.* 117:301–342.

Jørgensen, K., and O. G. Mouritsen. 1995. Phase separation dynamics and lateral organization of two-component lipid membranes. *Biophys. J.* 69:942–954.

Korlach, J., P. Schwille, W. W. Webb, and G. B. Feigensen. 1999. Characterization of lipid bilayer phases by confocal microscopy and fluorescence correlation spectroscopy. *Proc. Natl. Acad. Sci. USA.* 96: 8461–8466.

Koynova, R., and M. Caffrey. 1998. Phases and phase transitions of the phosphatidylcholines. *Biochim. Biophys. Acta.* 1376:91–145.

Lewis, R. N. A. H., N. Mark, and R. N. McElhaney. 1987. A differential scanning calorimetric study of the thermotropic phase behavior of model membranes composed of phosphatidylcholines containing linear saturated fatty acyl chains. *Biochemistry.* 26:6118–6126.

Lewis, R. N. A. H., R. N. McElhaney, F. Österberg, and S. M. Gruner. 1994a. Enigmatic thermotropic phase behavior of highly asymmetric mixed-chain phosphatidylcholines that form mixed-interdigitated gel phases. *Biophys. J.* 66:207–216.

Lewis, R. N. A. H., R. N. McElhaney, M. A. Monck, and P. R. Cullis. 1994b. Studies of highly asymmetric mixed-interdigitated gel phases: Fourier transform infrared and ^{2}H-NMR spectroscopic studies of hydrocarbon chain conformation and orientational order in the liquid-crystalline state. *Biophys. J.* 67:197–207.

Li, S., Z.-Q. Wang, H.-N. Lin, and C. Huang. 1993. Energy-minimized structures and packing states of a homologous series of mixed-chain phosphatidylcholines: a molecular mechanics study on the diglyceride moieties. *Biophys. J.* 65:1415–1428.

Li, S., Z.-Q. Wang, H.-N. Lin, and C. Huang. 1994. On the main phase transition temperatures of highly asymmetric mixed-chain phosphatidylcholines. *Biochim. Biophys. Acta.* 1194:271–280.

Lin, H.-N., Z.-Q. Wang, and C.-H. Huang. 1990. Differential scanning calorimetry study of mixed-chain phosphatidylcholines with a common molecular weight identical with diheptadecanoyl phosphatidylcholine. *Biochemistry.* 29:7063–7072.

Lin, H.-N., Z.-Q. Wang, and C.-H. Huang. 1991. The influence of acyl chain-length asymmetry on the phase transition parameters of phosphatidylcholine dispersions. *Biochim. Biophys. Acta.* 1067:17–28.

Mabrey, S., and J. Sturtevant. 1978. High-sensitivity differential scanning calorimetry in the study of biomembranes and related model systems. *In* Methods in Membrane Biology. Vol. 9. E. D. Korn, editor. Plenum Press, New York. 237–274.

Marčelja, S. 1974. Chain ordering in liquid crystals. II. Structure of bilayer membranes. *Biochim. Biophys. Acta.* 367:165–176.

Marsh, D. 1990. Handbook of Lipid Bilayers. CRC Press, Boca Raton, FL. 199.

Marsh, D. 1992. Analysis of the bilayer phase transition temperatures of phosphatidylcholines with mixed chains. *Biophys. J.* 61:1036–1040.

Marsh, D. 1999. Thermodynamic analysis of chain-melting transition temperatures for monounsaturated phospholipid membranes: dependence on *cis*-monoenoic double bond position. *Biophys. J.* 77:953–963.

Marsh, D., A. Watts, and I. C. P. Smith. 1983. Dynamic structure and phase behavior of dimyristoylphosphatidylethanolamine bilayers studied by deuterium nuclear magnetic resonance. *Biochemistry.* 22:3023–3026.

Mason, J. T., C. Huang, and R. L. Biltonen. 1981. Calorimetric investigations of saturated mixed-chain phosphatidylcholine bilayer dispersions. *Biochemistry.* 20:6086–6092.

Mattai, J., P. K. Sripada, and G. G. Shipley. 1987. Mixed-chain phosphatidylcholine bilayers: structure and properties. *Biochemistry.* 26: 3287–3297.

McIntosh, T. J., S. A. Simon, J. C. Ellington, Jr., and N. A. Porter. 1984. New structural model for mixed-chain phosphatidylcholine bilayers. *Biochemistry.* 23:4038–4044.

McMullen, T. P., R. N. A. H. Lewis, and R. N. McElhaney. 1999. Calorimetric and spectroscopic studies of the effects of cholesterol on the thermotropic phase behavior and organization of a homologous series of linear saturated phosphatidylethanolamine bilayers. *Biochim. Biophys. Acta.* 1416:119–134.

Melchior, D. L., and J. M. Stein. 1976. Thermotropic transitions in biomembranes. *Annu. Rev. Biophys. Bioeng.* 5:205–238.

Mendelsohn, R., M. A. Davies, J. W. Brauner, H. F. Schuster, and R. A. Dluhy. 1989. Quantitative determination of conformational disorder in the acyl chains of phospholipid bilayers by infrared spectroscopy. *Biochemistry.* 28:8934–8939.

Meraldi, J. P., and J. Schlitter. 1981a. A statistical mechanical treatment of fatty acyl chain order in phospholipid bilayers and correlation with experimental data. I. Theory. *Biochim. Biophys. Acta.* 645:183–192.

Meraldi, J. P., and J. Schlitter. 1981b. A statistical mechanical treatment of fatty acyl chain order in phospholipid bilayers and correlation with experimental data. II. Dipalmitoyl-3-sn-phosphatidylcholine. *Biochim. Biophys. Acta.* 645:193–210.

Morrow, M. R., J. P. Whitehead, and D. Lu. 1992. Chain-length dependence of lipid bilayer properties near the liquid crystal to gel phase transition. *Biophys. J.* 63:18–27.

Mouritsen, O. G., and R. L. Biltonen. 1993. Protein-lipid interactions and membrane heterogeneity. *In* Protein-Lipid Interactions. A. Watts, editor. Elsevier, Amsterdam. 1–39.

Mouritsen, O. G., A. Boothroyd, R. Harris, N. Jan, T. Lookman, L. MacDonald, D. A. Pink, and M. J. Zuckerman. 1983. Computer simulation of the main gel-fluid phase transition of lipid bilayers. *J. Chem. Phys.* 79:2027–2041.

Mouritsen, O. G., J. H. Ipsen, K. Jørgensen, M. M. Sperotto, Z. Zhang, E. Corvera, D. P. Fraser, and M. J. Zuckermann. 1992. Computer simulation of phase transitions in nature's preferred liquid crystal: the lipid bilayer membrane. *In* Computer Simulation of Liquid Crystals. G. F. Luckhurst, editor. Kluwer Academic Publishers, Dordrecht, The Netherlands.

Nagle, J. F. 1973. Theory of biomembrane phase transitions. *J. Chem. Phys.* 58:252–264.

Nagle, J. F. 1980. Theory of the main lipid bilayer phase transition. *Annu. Rev. Phys. Chem.* 31:157–195.

Nagle, J. F. 1993. Area/lipid of bilayers from NMR. *Biophys. J.* 64: 1476–1481.

Nagle, J. F., and D. A. Wilkinson. 1978. Lecithin bilayers: density measurements and molecular interactions. *Biophys. J.* 23:159–175.

Owicki, J. C., M. W. Springgate, and H. M. McConnell. 1978. Theoretical study of protein-lipid interactions in bilayer membranes. *Proc. Natl. Acad. Sci. USA.* 75:1616–1619.

Pearson, R. H., and I. Pascher. 1979. The molecular structure of lecithin dehydrate. *Nature.* 281:499–501.

Petrache, H. I., K. Tu, and J. F. Nagle. 1999. Analysis of simulated NMR order parameters for lipid bilayer structure determination. *Biophys. J.* 76:2479–2487.

Pink, D. A. 1982. Theoretical models of phase changes in one- and two-component lipid bilayers. *In* Biology Membranes. Vol. 4. D. Chapman, editor. Academic Press, New York. 131–178.

Pink, D. A., T. J. Green, and D. Chapman. 1980. Raman scattering in bilayers of saturated phosphatidylcholines. Experiment and theory. *Biochemistry.* 19:349–356.

Priest, R. G. 1980. Landau phenomenological theory of one and two component phospholipid bilayers. *Mol. Cryst. Liq. Cryst.* 60:167–184.

Sabra, M. C., and O. G. Mouritsen. 1998. Steady-state compartmentalization of lipid membranes by active proteins. *Biophys. J.* 74:745–752.

Salem, L. 1962. Attractive forces between long saturated chains at short distances. *J. Chem. Phys.* 37:2100–2113.

Schindler, H., and J. Seelig. 1975. Deuterium order parameters in relation to thermodynamic properties of a phospholipid bilayer. A statistical mechanical interpretation. *Biochemistry.* 14:2283–2287.

Seelig, J., and W. Niederberger. 1974. Deuterium-labeled lipids as structural probes in liquid crystalline bilayers. A deuterium magnetic resonance study. *J. Am. Chem. Soc.* 96:2069–2072.

Seelig, A., and J. Seelig. 1974. The dynamic structure of fatty acid acyl chains in a phospholipid bilayer measured by deuterium magnetic resonance. *Biochemistry.* 13:4839–4845.

Seelig, J., and A. Seelig. 1980. Lipid conformation in model membranes and biological membranes. *Q. Rev. Biophys.* 13:19–61.

Shah, J., P. K. Sripada, and G. C. Shipley. 1990. Structure and properties of mixed-chain phosphatidylcholine bilayers. *Biochemistry.* 29: 4254–4262.

Simons, K., and E. Ikonen. 1997. Functional rafts in cell membranes. *Nature.* 387:569–572.

Singer, S. J., and G. L. Nicolson. 1972. The fluid mosaic model of the structure of cell membranes. *Science.* 175:720–731.

Stümpel, J., H. Eibl, and A. Nicksch. 1983. X-ray analysis and calorimetry on phosphatidylcholine model membranes—the influence of length and position of acyl chains upon structure and phase behavior. *Biochim. Biophys. Acta.* 727:246–254.

Sugár, I. P., and G. Monticelli. 1985. Interrelationships between the phase diagrams of the two-component phospholipid bilayers. *Biophys. J.* 48: 283–288.

Sugár, I. P., T. E. Thompson, and R. L. Biltonen. 1999. Monte Carlo simulation of two-component bilayers: DMPC/DSPC mixtures. *Biophys. J.* 76:2099–2110.

Thompson, T. E., M. B. Sankaram, R. L. Biltonen, D. Marsh, and L. C. Vaz. 1995. Effects of domain structure on in-plane reactions and interactions. *Mol. Membr. Biol.* 12:157–162.

Tu, K., D. J. Tobias, and M. L. Klein. 1995. Constant pressure and temperature molecular dynamics simulation of a fully hydrated liquid crystal phase dipalmitoylphosphatidylcholine bilayer. *Biophys. J.* 69: 2558–2562.

van der Ploeg, P., and H. J. Berendsen. 1982. Molecular dynamics simulation of a bilayer membrane. *J. Chem. Phys.* 76:3271–3276.

Wang, Z.-Q., H.-N. Lin, and C.-H. Huang. 1990. Differential scanning calorimetry study of a series of fully hydrated saturated mixed-chain C(X):C(X+6) phosphatidylcholines. *Biochemistry.* 29:7072–7076.

Xu, H., and C. H. Huang. 1987. Scanning calorimetric study of fully hydrated asymmetric phosphatidylcholines with one acyl chain twice as long as the other. *Biochemistry.* 26:1036–1043.

Yellin, N., and I. W. Levin. 1977. Hydrocarbon chain trans-gauche isomerization in phospholipid bilayer gel assemblies. *Biochemistry.* 16: 642–647.

Zhu, T., and M. Caffrey. 1994. Thermodynamic, thermomechanical, and structural properties of a hydrated asymmetric phosphatidylcholine. *Biophys. J.* 65:939–954.